k_o – NAA EVALUATION OF Al /Si CONCENTRATION RATIOS IN BAUXITES USING 5Ci AM-Be NEUTRON SOURCE IRRADIATION FACILITY.

BY

SULEIMAN SHAIBU ASUKU B.Sc (ABU 2004)
M.Sc /SCIE/49554/05-06

A thesis submitted to the postgraduate school, Ahmadu Bello University, Zaria, in partial fulfillment of the requirement for the award of the degree of Master of Science (M.Sc) in physics.

DEPARTMENT OF PHYSICS,
AHMADU BELLO UNIVERSITY, ZARIA,
NIGERIA.

MAY, 2011

DECLARATION

I declare that this project/ thesis entitled "ko–NAA evaluation of Al/Si concentration ratios in bauxites using 5Ci Am-Be neutron source irradiation facility" is my own work and has not been submitted in any form for another degree or diploma to any other University or Institution. Information derived from published or unpublished work of other workers has been acknowledged in the text.

_____ _____

Suleiman Shaibu Asuku Date

CERTIFICATION

This thesis "ko-NAA Evaluation of Al/Si Concentration Ratios in Bauxite using 5Ci Am-Be Neutron Source Irradiation Facility" by Suleiman Shaibu Asuku meets the regulations governing the award of the degree of Master of Science in Physics of Ahmadu Bello University, Zaria and is approved for its contribution to knowledge and literary presentation.

Dr. Nasiru R. Chairman, Supervisory Committee	Date
Prof. S.A Jonah. Member, Supervisory Committee	Date
Dr. Nasiru R. Head, Dept of physics	Date
Prof. Joshua A.A. Dean, Postgraduate School	Date

DEDICATED

This work is dedicated to Allah (S. W. T) and the seal of all His Prophets, Muhammad bn Abdullah (S. A. W).

ACKNOWLEDGEMENTS

Glory and thanks be to Allah, the most high and dignified, with whose wish I am at this level of my academic pursuit. May His peace and blessings be upon prophet Muhammad (SAW).

I thank my supervisors, Dr. Nasiru Rabiu and Prof. S.A Jonah for being patient with me and taking their time to read the work and make corrections despite their tight schedules.

To all the staff of physics Department, I say thank you for your advice and encouragement. I am grateful to the Director and staff of the Centre for Energy Research and Training, CERT, ABU-Zaria for allowing me access to their facilities. I also appreciate Geology and chemistry Departments for their assistance.

I am strongly indebted to my mother, Hajiyah Suleiman Munirat for her prayers, support and encouragement and my dear wife Shuaibu Ruqayyah- your love, patience, support, understanding and encouragement is highly acknowledged. Thanks for being there for me all through.

To my only brother Alhaji Suleiman Ibrahim, I am indeed grateful for your advice and financial support. I also appreciate all my sisters and in-laws for their efforts.

My guardian, Hajiyah Omenesa SCA/DAC ABU-Zaria, I say thank you for your moral and financial supports.

To all my friends, colleagues and well-wishers, thanks for your support, care and love.

This acknowledgement will be incomplete if I fail to mention my late father, Suleiman Anate and my late Mallam, Sheikh Abdallah Gaminana, may Allah have mercy on your souls.

ABSTRACT

An irradiation method with thermal and fast neutrons from a 5Ci Am-Be neutron source facility in combination with 3"x3" NaI(Tl) detector system has been used to determine Al/Si concentration ratios in alumino-silicate ores via K_0-NAA. Two different samples were analyzed; raw bauxite samples from exploration field and other bauxite samples from the NAA Laboratory of CERT - A.B.U Zaria. Samples were co-irradiated bare and under cadmium-cover with gold foil as a monitor for one hour and counted for ten minutes. One minute delay was observed for the samples and 13minutes for the foils before counting. The peak area analysis of the 1779Kev and 411.8Kev gamma-ray lines of ^{28}Al and ^{198}Au product radionuclides produced via $^{27}Al(n,\gamma)^{28}Al$ and $^{197}Au(n,\gamma)^{198}Au$ reactions respectively, the flux ratio, f, the flux shapping parameter, α of the irradiation sites and the K_0-values for $^{27}Al(n,\gamma)^{28}Al$ and $^{197}Au(n,\gamma)^{198}Au$ reaction were used to determine the aluminium concentration in the samples. Due to unavailability of K_0- Value for $^{28}Si(n,p)^{28}Al$, the peak counts of ^{28}Al product radionuclide produced via $^{27}Al(n,\gamma)^{28}Al$ and $^{28}Si(n,p)^{28}Al$ reactions, the neutron flux in the irradiation sites, the neutron cross-section for (n,γ), (n,p) reactions and the aluminium concentrations obtained via k_o-NAA were used to determine silicon concentration in the samples. Our results (11.13±1.15%, 8.09±0.75%, 0.021±0.007%) compare well with the results obtained from the Reactor Neutron Activation Analysis (RNAA) for aluminium concentration in the raw samples. The Al/Si concentration ratios evaluated for other samples are; 0.72±0.05, 0.98±0.14, 0.97±0.12, 0.70±0.11, 0.98±0.14, 0.59±0.03, 0.67±0.08, 0.57±0.08, 0.67±0.07, 0.84±0.05, 0.38±0.07, 0.41±0.01, 0.81±0.05, 1.30±0.25, 0.55±0.27. These ratios compare well with the results of earlier analysis done on

them using a different approach (Jonah et al, 2004). Our results show that k_0-NAA evaluation of Al/Si concentration ratio in alumino-silicate ores is achievable.

CONTENTS

Title page - - - - - - - - - i

Declaration - - - - - - - - - ii

Certification - - - - - - - - iii

Dedication - - - - - - - - - iv

Acknowledgement - - - - - - - - v

Abstract - - - - - - - - - vi

Contents - - - - - - - - vii

CHAPTER ONE - - - - - - - - 1

1.0 General Introduction - - - - - - - 1

1.1 Neutron Activation Analysis (NAA) Technique - - - - 2

1.1.1 K_0-Neutron Activation Analysis (K_0-NAA) Method - - - 2

1.2 Previous Works - - - - - - - - 4

1.3 Motivation of the Work - - - - - - - 5

1.4 Aims and Objectives - - - - - - - 6

CHAPTER TWO - - - - - - - - 7
2.0 Review of Related Literatures - - - - - - 7

2.1 Neutron Interaction with Matter - - - - - - 7

2.1.1 Absorption - - - - - - - - 7

2.1.2 Scattering Process - - - - - - - 8

2.1.3 Classification of Neutrons - - - - - - 9

2.1.4 Neutron Reaction Cross-Section - - - - - 9

2.1.5 Neutron Sources - - - - - - - 11

2.1.6 Am-Be Neutron source - - - - - - - 11

2.2 Theory of Activation Analysis - - - - - - 12

2.2.1 Mechanism of Hogdhl's convention - - - - - 22

2.2.2 Neutron self shielding and Cd transmission factor - - - 22

2.2.3 Activation equation - - - - - - - 23

2.2.4 Principles of standardization - - - - - - 24

2.2.5 Relative standardization - - - - - - 25

2.2.6 Absolute method - - - - - - - 27

2.2.7 The Single Comparator Method - - - - - 27

2.2.8 The K_0 – standardization - - - - - - 28

2.2.9 Geology of Bauxites - - - - - - - 29

2.3.0 Economic importance of Bauxites - - - - - 31

CHAPTER THREE - - - - - - - - 34

3.0 Materials and Methodologies - - - - - - 34

3.1 Sample collection - - - - - - - - 34

3.1.1 Brief Geography of the Mambilla Plateau - - - - 34

3.1.2 Sample Preparation- - - - - - - - 34

3.1.3 Sample preparation for irradiation using ^{241}Am-Be Neutron source - - 35

3.2.0 Experimental set-up - - - - - - - 36

3.2.1 ^{241}Am-Be Neutron source irradiation facility - - - - 36

3.2.2 Sodium Iodide Thallium activated [NaI(Tl)] detector - - - 37

3.3.0 Experimental procedures - - - - - - 39

3.3.1 Energy Calibration - - - - - - - 39

3.3.2 Absolute Efficiency Calibration - - - - - 39

3.3.3 Efficiency Calibration for Bulk Sample - - - - 41

3.3.4 Measurement of Detection Limit (L_D) and Detectable mass (M_D) - - - 42

3.3.5Sample Irradiation and Counting - - - - - 43

3.3.6 Determination of Aluminium Concentration via ko-NAA - - - - 44

3.3.7 Determination of Silicon Concentration - - - - - - - - - 45

CHAPTER FOUR - - - - - - - - - 50

4.0 Results and Discussions - - - - - - - 50

4.1 Results of Calibration - - - - - - - 50

4.1.1 Energy Calibration - - - - - - - 50

4.1.2 Efficiency Calibration - - - - - - - 50

4.2 Limit of Detection (L_D) and Detectable mass (M_D) - - - - 51

4.3 Determination of Aluminium concentration in the Samples - - - 52

4.4 Determination of Silicon Concentration - - - - - 52

CHAPTER FIVE - - - - - - - - 68

5.0 Summary, Conclusion and Recommendation - - - - 68

5.1 Summary - - - - - - - - - 68

5.2 Conclusion - - - - - - - - 68

5.3 Limitation and Recommendation - - - - - - -- 69

References - - - - - - - - - 72

CHAPTER ONE

1.0 GENERAL INTRODUCTION

The discovery of a chargeless particle, the neutron by James Chadwick opened the gate to a better understanding of matter. This discovery led to the development of valuable technique used in the analysis of matter known as Neutron Activation Analysis (NAA). This Technique has attained tremendous height of improvement in analysis of biological, chemical and geological samples. The present technological advancement in industries has led scientist to think of new and more efficient method of exploration, extraction, processing and grading of geological ores. This is evident from the fact that the world is endowed with abundance mineral resources and also the rapid growth in world's mineral consumption. The use of more sophisticated processes and their effective control is an important aspect of increasing efficiency. Conventional chemical method is tedious and no longer economical. Nuclear techniques, more especially neutron activation analysis (NAA) have become important for routine measurement of elemental concentration and for process control in bulk material because of their higher penetrating ability (Minxhozi, 1982). A study conducted at the United State Geological Survey Denve Geochemical Laboratory showed that from 1978 to 1983 the number of determinations by all methods rose from 66,000 samples per year to 137,000 samples per year with corresponding increase in elemental determination per sample from 5-13 (Taggent, 1984). The ability of nuclear techniques to perform rapid and accurate, non-destructive analysis over a wide range of concentration was observed to be the key to this success.

1.1 NEUTRON ACTIVATION ANALYSIS (NAA) TECHNIQUE

This technique involve the bombardment (irradiation) of a target (material or substance whose component or composition we wish to analyse) with neutrons where upon a radionuclide is formed which can be quantified using nuclear measurement technique (Kruger, 1971, Socte, et al, 1972). The artificial radionuclide (irrespective of how it is produced) is unstable and will always decay with characteristics half – life and radiation emission having characteristics energy or energies. These two parameters (half – life and energy) determine uniquely the radionuclide in question, thus providing a specific basis for elemental identification.

Gieger Muller (G.M) counters were used to measure the induced activities at the early stage of its development. The introduction of sodium lodided Tallium activated [NaI (Tl)] scintillation detector, Germanium Lithium drifted (GeLi,) detector and High Purity Germanium (HPGe) detector in gamma spectroscopy together with a single or multichannel analyzer serve as a major break through in N.A.A. technique. With the above development, it is possible to analyse over forty elements in a sample matrix.

Other advantages of neutron activation analysis particularly with isotopic neutron source over conventional chemical methods include, the great reduction of labour and time consumption in sampling and sample preparations. Sample size are usually large (ten to a few hundred grams), analytical results are available quickly enough for effective process control and the method is easily automated (Bardossy and White, 1980, Clayton, 1982). Use of this technique in the determination of aluminum and other elements in bauxite with a very good accuracy has been widely reported (Weiss et al, 1978, Garge and Batra, 1986, Hoste, 1988)

1.1.1 K_O–NEUTRON ACTIVATION ANALYSIS (K_O – NAA) METHOD

The Ko-Method is a single – comparator standardization protocol for Neutron Activation Analysis (NAA). The method is widely accepted for multi-element Neutron Activation Analysis with research reactor because it allows flexibility with respect to variation in neutron spectrum parameters and gamma ray counting geometry. The rate of production of radioactive atoms of interest (as observed with a gamma-ray detector) is related to activation rate of gold through the so–called K_o–constant. This relative production rate depends on the specific irradiation facilities and gamma ray detectors used. The method therefore also presents how to determine the required characteristics of the irradiation facility and the detector. This "single–comparator" method has been critically evaluated and it was proven that it is as accurate as the relative standardization.

The K_o–constants is defined for the simplest activation decay type as

$$K_0 = \frac{M_c \theta_a \sigma_a \gamma_a}{M_a \theta_c \sigma_c \gamma_c}$$

Where a and c denote analyte and comparator respectively

M_c = atomic mass (g/mol)

σ = thermal neutron cross –section

θ = isotopic abundance

γ = absolute gamma–ray abundance

This constant represent the relative production rate or rather the part of that rate that is independent of irradiation facility and detector, and plays an essential part in the computation of concentration in K_o–NAA. The constituents of the constant could be found in literature separately, but in some cases with poor reliability. The Ko–constants were therefore measured directly in some specialized institutes; at the Institute of Nuclear Sciences in Ghent, at RISO in Denmark.

Knowing the k_o–constants, once the irradiation facility and the detector have been characterize, each sample needed to be Co–irradiated with a gold comparator only, rather than with as many comparators (or standards) as there are elements to be determined in the sample. Errors in the preparation of standards are thus excluded. In exchange, systematic errors in the k_o–constants will affect all the results obtained. These errors have been shown to be small, however. The general agreement is that the errors in the constants are smaller than 3.5%. Sample and gold comparator may have different shapes, neutron and gamma absorption characteristics. Correction procedures for these differences are also considered to be integral parts of the k_o–method. The k_o–factor for many nuclides have been determined and published in a joint project involving the Activation Analysis Laboratory of the Central Research Institute for Physics in Budapest and Institute for Nuclear Sciences in Ghent using gold as a comparator.

1.2 PREVIOUS WORKS

Instrumental neutron activation analysis techniques have been used for several elemental analysis, process control and mineralogical analysis both local and at international level. The work include, the determination of concentration of tantalum in its Ore containing mineral using a 5Ci Pu–Be neutron source (Gurner and Bhalla, 1977). Fast neutrons from 5Ci ^{241}Am-Be neutron source were used to determine iron and silicon in USGS, Indian standard and bauxites by cutting off thermal neutron with a cadmium shield (Betra, et al, 1986). The same method has been used for the

determination of iron and silicon in their alloys, ores and coal (Betra, et al (1986). It was observed that isotopic neutron source (INS) have constant neutron flux provided the facility is kept unchanged, this make it possible the use of isotopic neutron source for the determination of precious and rare metals in their Ore deposits via k_o–standardization method (Hoste; 1988). Elemental analysis of copper in its Ore was carried out using 5Ci $^{241}Am-Be$ neutron source (Batra and Garg; 1989). ^{241}Am–Be thermal neutron source with a flux of 1.7 x 10^7neutrons/cm.sec was used in gold prospecting in Ghana (Ahmad, et al; 1991) indium and tin have been determined from tin Ore (Cassiterite) using Instrumental Neutron Activation Analysis (INAA) (Illa and MacFarlane; 1991). A 5Ci $^{241}Am-Be$ isotopic neutron source was installed at the Centre for Energy Research and Training (CERT) ABU Zaria in Nigeria and so far a lot of research works on elemental analysis have been done. These include; the determination of manganese in manganese Ore deposits using the 5Ci $^{241}Am-Be$ isotopic neutron source (INS) (Onojah, 1995) Determination of aluminum in bauxite ore using the same isotopic neutron source present at the CERT (Idris, 1998). The determination of the total hydrogen content of the Nigeria commercial oils using INS was done at the CERT (Jonah, el al; 1999) Epithermal neutron parameters of the irradiation sites have been determined for the facility present at the Centre for Energy Research and Training ABU–Zaria (Mustafa, el al; 2003). Recently, the determination of copper and gold in their respective ores using k_o-standardized method of Neutron Activation Analysis with 5Ci $^{241}Am-Be$ neutron irradiation facility at the Centre for Energy Research and Training was carried out (Rabiu, 2005).

1.3 MOTIVATION OF THE WORK

Since after the discovery of neutron in 1932, the subsequent development of the technique of Neutron Activation Analysis (NAA) and more recently the launch of k_0–method and its standardization, elemental analysis have become easier, this is not only in terms of easy sample preparation, availability of results within a short period but also in terms of non-destructive nature of the method, concise and precise nature of the method, multi elemental analysis (analyzing over ten elements per sample) and its application in different research fields among others. It finds application in forensic science, geology, biology, archaeology, authentication of works of art and in general industry.

The successes recorded in the previous works reviewed made us to choose the method using the k_o–Neutron Activation Analysis (k_o–NAA) approach to carry out this research work. More importantly, the alumina content of bauxite determine its value grade and industrial usefulness, an improved and accurate analysis of alumina content is of great importance in bauxite exploration as well as in aluminum industry. This necessitates the need to develop rapid, accurate and non–destructive method for the evaluation of Alumino-Silicate concentration ratio in bauxite ore which is the subject of this work.

1.4 AIMS AND OBJECTIVES OF THE WORK

This work is aimed at performing the following tasks

i. The characterization of the gamma ray spectrometry system

ii. The determination of the concentration of aluminum and silicon in raw bauxite samples via k_o-NAA

iii. The determination of alumino-silicate concentration ratio of other samples of bauxites via k_o-NAA

iv. Comparing the ratios with the result obtain from Reactor Neutron Activation Analysis (RNAA) .

CHAPTER TWO

2.0 REVIEW OF RELATED LITERATURE

2.1 NEUTRON INTERACTION WITH MATTER

The manner in which neutrons interact with matter and their energies are of prime concern in neutron activation analysis (NAA). By definition, neutrons are elementary particles of atom with mass number 1, half life of 12min. It has no electrical charge with high penetrating power. A neutron has a rest mass of 1.008665U. (where U is the atomic mass unit), has half integral spin, obeys Fermi Dirac statistics and possesses a negative magnetic moment of -1.9103nuclear magneton (Taylor and Havens,1949). The electrical neutral character of the neutron makes it pass through matter more readily than charged particles.

It approaches or enters nucleus without having to overcome the repulsive coulomb force. This is why a high velocity is not a prerequisite for neutron reaction to take place as it is the case with charged particles. In fact, fast neutrons are less effective in producing certain nuclear reaction. The process of neutron interaction with matter are classified into absorption and scattering.

2.1.1 ABSORPTION

In absorption reaction, a neutron enters a nucleus, thereby forming a new nucleus that has been raised (excited) to a high energy-state which is commonly referred to as compound nucleus. This compound nucleus being extremely unstable de-excites within about 10^{-12} seconds or less (IAEA, 1970) and gets rid of its excess energy by emitting gamma ray or heavy charged particle provided the neutron energy is high enough. This is because nature always seeks its lowest energy level or state (i.e. ground state). The most common nuclear reaction under this category is the (n, γ) reaction.

This is otherwise known as radioactive capture. Others like (n,p), (n,α) reactions are also possible if the neutron energy is high. In (n,n) process, the emitted particle is also a neutron with much lower energy than the captured neutron. The overall effect is that a colliding neutron transfers its kinetic energy to the target, all of which is expended as gamma radiation emitted from the compound nucleus. This is why the (n,n) reaction is usually called inelastic scattering. In fact, since there is no net loss of neutrons in this type of reaction, it is generally not included in the discussion of neutron absorption processes (IAEA, 1970).

2.1.2 SCATTERING PROCESS

This happens when a neutron collides with a nucleus of the target and transfer all or parts of its energy to it without being absorbed by the target. Scattering may be elastic or inelastic, depending on whether the neutron energy is partly spent on exciting the target nucleus or is transferred to the target without changing form. We have explained the inelastic scattering in the (n,n) capture reaction described above.

Elastic scattering is the dominant mode of interaction of neutron with matter for the neutron with energies in the range 10eV-10MeV (Mossop, 1963). In this process the neutron kinetic energy is partially transferred to the target nucleus, thereby becoming slow down, consequently, the direction is changed because of the collision it made with the target nucleus. The amount of energy that can be transferred depends only on the mass of the nucleus participating in the collision, the smaller the participating nucleus, the greater the energy that can be transferred. Since both kinetic energy and momentum are to be conserved in elastic scattering process, the maximum possible energy resulting from a head-on-collision is:

$$E_1 - E_2 = \frac{4A}{(A+1)^2} E_1 \quad \text{.....2.1}$$

Where E_1 is the energy of the neutron before collision, E_2 is the energy of the neutron after collision, A is the relative atomic weight of the nucleus which can be considered equal to its mass number, the relative atomic mass of the neutron can lose all its kinetic energy in a single head-on collision with hydrogen nucleus (i.e. A = 1). This is why water, paraffin and other hydrogenous substances are used as neutron moderators.

2.1.3 CLASSIFICATION OF NEUTRONS

Since neutron do not carry any electric charge, they can not be accelerated by any field but can only be moderated. That is, they can only be stopped or slow down by collision with other particles. Neutrons are classified based on their energies as; Thermal neutrons (energy of about 0.025eV), epithermal neutrons (energy of about 0.2eV): Cadmium neutrons (energy of about 0.6eV); Slow neutrons (energy of about 1-10eV); resonance neutron (a wide range of energies 1.-300eV); middle neutron (energy of about 500eV-0.5MeV) and ultra fast (energy of above 20MeV). Fission neutrons are those present in a reactor which has not been moderated. They are called reactor neutrons with energy spectrum from 0.001eV-15MeV (Rakovich, 1970).

2.1.4 NEUTRON REACTION CROSS-SECTION

A reaction cross-section is a nuclear property of any given isotope that is proportional to the probability of its nucleus to undergo a given type of nuclear reaction. When only one single nucleus is involved, its cross-section is known as 'microscopic cross-section' it is denoted as $\sigma(x,i)$. The suffixes refer to the type of reaction and a type of nucleus respectively. Cross-section is not related to the actual physical size of the nucleus. It has unit of area usually expressed in barns and a barn is defined as $10^{-24}cm^2$(IAEA, 1970).

The chances of occurrence of any type of neutron reaction depend both on the energy of the neutron and the nature of the nucleus. When a medium is considered, the total cross-section of its nuclei in a unit volume is called "Macroscopic cross-section", denoted by $\sum$. generally defined as

$$\sum = N\sigma \times 10^{-24} cm^2 \quad \text{.....2.2}$$

Where σ is in barns for the corresponding type of reaction, N is the total number of nuclei in a unit volume (i.e. in cm^3). Since we can get N from Avogadro's number, the macroscopic cross-section for a medium of only one type of isotope is

$$\sum = \frac{\rho N_A \sigma \times 10^{-24}}{A} = \frac{0.602\rho\sigma}{A} cm^{-1} \quad \text{.....2.3}$$

Where A is the mass number of the isotope, ρ is the density of the medium in g/cm^3. In most cases, the value σ is usually given for an element, not for its particular isotopes. In such a case, equation 2.3 above is only valid if A is taken as the atomic weight of the element and $\sum$ is then the macroscopic cross section of the material (IAEA, 1970).

But in practice, the medium of interest is composed of several elements. Assuming such medium to be homogeneous, the cross-section for a given type of reaction at certain energy is the weighted contributions of the entire element present. The general equation for medium comprising m element is

$$\sum = N_1\sigma_1 + N_2\sigma_2 + ... + N_m\sigma_m \quad \text{.....2.4}$$

$$= \sum_{i=1}^{i=m} N_i\sigma_i \quad \text{.....2.5}$$

Where N_i is the number of nuclei of element i in one cm^3 of the medium and σ_i represent its microscopic cross-section (IAEA, 1970). Now supposing that the weighted percentage ω_i of each constituent element is known, and then the equation becomes

$$\sum = 6.02x10^{-3}\rho\sum_{i=1}^{i=m}\frac{\omega_i\sigma_i}{A_i} \quad \ldots\ldots\ldots\ldots\ldots\ldots\ldots\ldots\ldots\ldots\ldots\ldots\ldots\ldots 2.6$$

2.1.5 NEUTRON SOURCES

There are three main types of neutron sources for activation analysis. These are neutron generators, isotopic neutron sources and nuclear reactor. Others include charged particle sources. The choice of neutron source depends on the problem to be solved. Whenever a high sensitivity is required, a research nuclear reactor or even a high flux reactor is required. If oxygen is to be determined, a 14MeV neutron generator is most appropriate because of the high threshold energy (about 9MeV) of the most useful reaction $^{16}O(n,p)^{16}N$. The determination of fluorine content of fluorine ores and concentrate through the $^{19}F(n,\alpha)^{16}N$ (threshold energy of 2MeV) without interference from the $^{16}O(n,p)^{16}N$ reaction require an unmoderated isotopic neutron source (e.g Am-Be) as the best choice of neutron sources. Other criteria worthy of note are; cost of the neutron source, dimension of the sources including shields, transportation effect, availability of highly skilled personnel among others (IAEA, 1970). In mobile installations for geochemical prospecting, radioisotope sources with neutron yields less than 10^8 neutron/seconds with or without moderator have been reported (Gijbels and Hertogen, 1977) as the most frequently used, particularly in the former Soviet Union.

2.1.6 Am-Be NEUTRON SOURCE

The sources is made as a compact mixture of Americium oxide (AmO_2) and Beryllium metal powder, with Am having 1gm as the isotopic weight and Be having 10gm. It is normally 30mm in diameter and 50mm in height as regard to dimension. The container is made of Nickel and Stainless Steel material for inner and outer encasement. The compact making of this source raises the probability that physical composition of the source might changed slightly with time as the constituents shift relative to each other. This could in turn cause the neutron yield to change. Hence, the neutron emission rate should be calibrated periodically at least once in every five years (Hoste, 1988). The large half-life of ^{241}Am(about 433 years) make possible the fabrication of these sources of approximately constant neutron emission rate with a simple decay correction because of the very long half life of the daughter nucleus $^{237}Np(2.2x10^6\ years)$. Am-Be is an (α, n) neutron source.

The neutron yield and to a lesser extent, the spectrum source will change depending upon the physical considerations. If the atomic ratio of Be to Am is large $(\geq 200:1)$ and preferably 268: 1, maximum yield is achieved (Jordan and Schierling, 1964). The physical size of the source is largely determined by the amount of the target material and thus, there is a line between maximum neutron yield and maximum source size.

Neutrons are produced in the Am-Be source by $^9B(\alpha, n)^{12}C$ reaction. The reaction is exoergic with Q value of 5.703MeV and average kinetic energy of the alpha particle being 5.47MeV giving a total energy of about 11MeV. This appears as the excitation and recoil energy of the carbon-12 product and as the kinetic energy of the emitted neutron (DZhelepov, 1961). The maximum neutron emission rate of Am-Be source is 2.5 to 3.6 neutrons per 10^6 alphas for $5C_i$ source (Hoste, 1988). The neutrons produced here have wide energy spectrum which depends on the angle of scattering that is quite spread out with well established peaks at 3.3, 4.3 and 5.0MeV.

2.2 THEORY OF ACTIVATION ANALYSIS

Theoretically, activation analysis can be carried out by means of any radiation with sufficient energy to induce radioactive species when a target sample is exposed to the bombarding particles. In practice, thermal neutrons have hitherto been the most frequently used in N.A.A. where stable element is converted to a radionuclide by the (n,γ) process depicted below

$${}^{A}_{Z}X_{N}+n\rightarrow {}^{A+1}_{Z}X_{N+1}+\gamma$$ ……..2.7

Where X is the target nuclide, A, Z and N are the Mass, atomic and neutron number respectively, n is the bombarding neutron and γ is the gamma energy emitted.

Assuming a target with N nuclide per cm^3 is placed in a neutron flux, Φ (neutrons, $cm^{-2}S^{-1}$). Then the number of interactions per seconds is given by

$\Phi.\sigma.N\ (cm^{-3}S^{-1})$……..2.8

Where σ is the reaction cross-section and can be defined from equation 2.8 as

$$\sigma = \frac{\text{Number of interactions } (cm^{-3}S^{-1})}{\Phi(cm^{-2}S^{-1})N(cm^{-3})}$$ ……2.8

Therefore, the (n,p) reaction rate per nucleus (interaction per second) is given by;

$R = \Phi.\sigma$ ……2.10

In general, eqn 2.10 can be written in the form

$$R = \int_0^\infty \sigma(v)\phi(u)du = \int_0^\infty \sigma(E)\phi(E)dE \quad \text{.....2.11}$$

Where

$\sigma(v) = (n,\gamma)$ Cross-section at neutron velocity, v

$\sigma(u) = (n,\gamma)$ Cross-section at neutron energy, E

$\phi(v)$ = neutron flux per unit of velocity interval at neutron velocity, v

$\phi(E)$ = neutron flux per unit of energy interval at neutron energy, E.

We can rewrite eqn 2.11, $\sigma(u) = \sigma(E)$ with $E = \frac{1}{2} m_n V^2$,where m_n is the rest mass. It also follows that $\phi(u)du = \phi(E)dE$.

The function $\sigma(u) = \sigma(E)$ and $\phi(v) = \phi(E)$ are complex and they depend on the (n,γ) reactions and irradiation site respectively. Fortunately introduction of some generally valid characteristics yields the possibility of avoiding the real integration and of describing accurately, the reaction rate in a relatively easy way by means of the so called formalism or convention. In effect these characteristics are;

(i) The (n,γ) cross-section, σ(v) versus v has been shown to vary as $\frac{1}{v}$ (De Corte, 1987), that is σ(v) ~ $\frac{1}{v}$ dependence or σ(E) versus E as a σ(E) ~ $\frac{1}{E^{\frac{1}{2}}}$ dependence. Above the thermal energy region, the cross-section shows some complex behaviour known as resonance. This is illustrated in fig 2.1 below

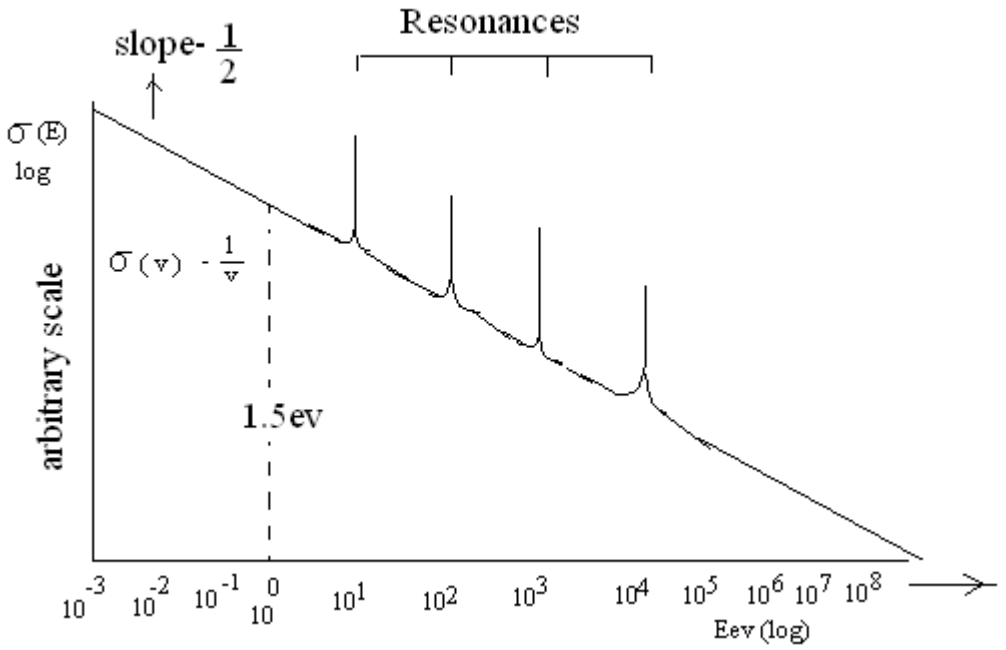


Fig 2.1: Schematic representation of (n, γ) cross section σ(E) vs E (De-Corte, 1987)

Within this resonance region, the cross-section obeys the Breit-Weigner one level formula (Breit and Weigner, 1936). It is important to note that only a few (n,γ) reactions of interest in NAA show significant deviation from the $\frac{1}{v}$-dependence in the energy region below 1.5eV (due to low-lying resonance). These deviations are accounted for by multiplying eqn2.11 by a factor $g(T_m)$, known as Wescott correction factor. The factor depends on neutron temperature T_n.

(ii) The neutron flux distribution $\phi(E)$ versus E is subdivided into three components (see fig2.2 below).

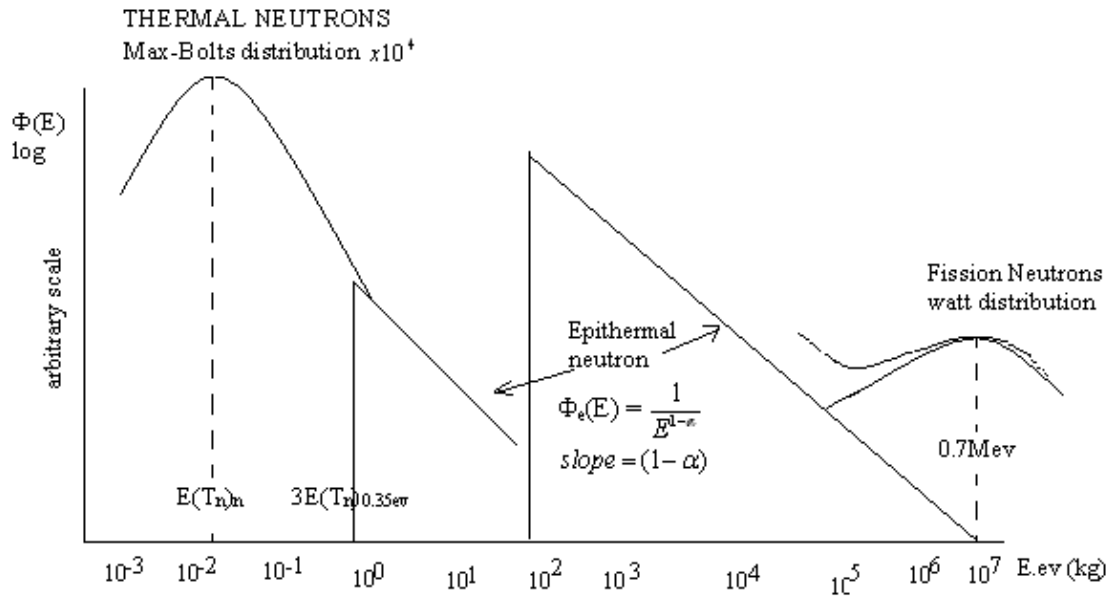


Fig2.2: $\phi(E)$ Versus E (De corte, 1987)

a) A fission (fast) neutron spectrum, which has a continuous energy distribution with a maximum higher than 10meV. They are described by Watt's empirical equation

$$n(E) = 0.7725E^{\frac{1}{2}} \exp(-0.775E) \quad \text{.....2.12 (Hoste, 1988)}$$

However, the contribution of this group of neutrons (above 1MeV), to (n, γ) reaction is usually small and may be ignored. They however give rise to threshold reactions e.g. (n,n), (n,p) (n,α) (n, 2n) and can cause interference as in the determination of Aluminium by the $^{27}Al(n,\gamma)^{28}Al$ reaction. Where the presence of silicon can give rise to positive error.

b) The thermal neutrons: These are low energy neutrons, They arise from successive collisions of high energy neutrons with the moderator atoms. This process is known as thermalisation. These neutrons which are in thermal equilibrium with atoms of the moderator obey Maxwell-Boltzmann distribution (IAEA, 1970). In $\phi(E)$ versus E or n(u) versus v curve, the most probable neutron energy at 20°C obtained from $E_n = kT$ is $\frac{1}{40}eV$ corresponding to neutron velocity of 220m/s. Different reaction conventions have been applied to described the reaction rate for (n, γ) reactions, such as those developed by Wescott (De Corte, 1987). However, the most practical version for activation analysis is the one proposed by HΦgdahl (De Corte, 1987 and Hoste, 1988) which is valid if

$$\sigma(v) \equiv \frac{1}{v} \quad \text{.....2.13}$$

This is the case for almost all nuclides of interest in activation analysis.

c) Epithermal neutrons: These are neutrons that loose energy by collision with moderator's atom but did not reach thermal equilibrium with the moderator. The spectrum in this case can be described by

$\phi(E) = \frac{1}{E}$ dependence……..2.14

However, in actual irradiation sites, eqn2.14 can be replaced by

$$\phi_e(E) = \frac{1}{E^{1+\alpha}} \text{ ……2.15}$$

Where α is greater or less than zero, being the first approximation, independent of neutron energy (De Corte, 1987). The neutron flux and reaction rate could be divided into two parts using a cadmium filter. Thus, a sample irradiated under cadmium is only activated by epithermal neutrons, the conventional maxwellian flux plus part of the epithermal flux up to the energy of cadmium cut-off. Thus by irradiating a nuclide under Cd-cover, the (n, γ) reaction is drastically reduced in the low energy region, where the neutrons are largely absorbed by the cadmium due to the very high cross-section of cadmium for (n,γ), resulting from the ^{113}Cd (n, γ) ^{114}Cd resonance at 0.178eV as observe in the fig2.3 below. The transmission function as function of energy under cadmium cover is shown in fig2.4. It is represented by

$$T(E) = \exp(-\sigma_{tot} Cd(E) \delta I_0 \frac{N_A}{M}) \text{……2.16}$$

Where σ_{tot} Cd = cross-section function (in cm^2)

δ = density of cadmium (8.642g/cm^3)

N_A = Avogadro's number ($6.023 \times 10^{23} mol^{-1}$)

I_o = Cadmium thickness (~0.1cm)

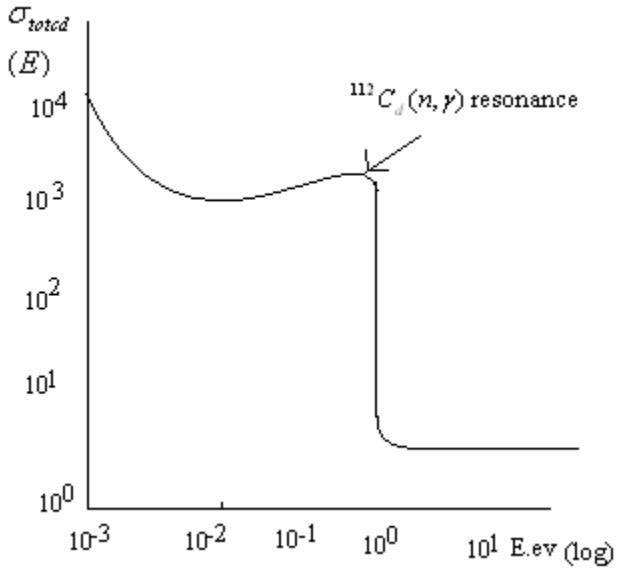


Fig 2.3: C_d Total cross section curve, σ_{totcd} vs E (De-Corte, 1987)

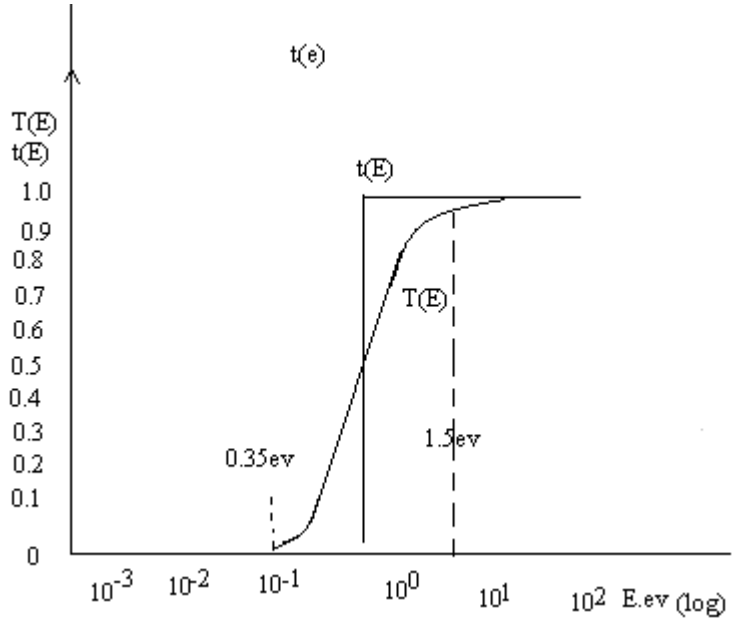


Fig 2.4: Actual and idealized Cd transmission, T(E) and t(E) vs E (De Corte, 1987).

It was assumed that the geometry effects caused by sample and cadmium cover were negligible in obtaining the T(E) curve. Also a mono directional beam of neutrons were assumed hitting a 0.1cm thick cadmium foil in a direction normal to its face. By defining an idealized transmission as a step function t(E), situated at the so called cadmium cut-off energy, E_d (with t(E) = 0 at E = E_d and t(E) = 1 at E > E_d), so that the epicadmium reaction rate R may be written as

$$R_e = \int_0^\infty \sigma(E)\phi(E)T(E)dE = \int_0^\infty \sigma(E)\phi(E)t(E)dE = \int_{E_{cd}}^\infty \sigma(E)\phi(E)dE \quad \text{.....2.17}$$

A value of 0.55eV has been internationally accepted as the standard value of E_{cd} under the following conditions:

i The irradiated material should have a relatively small volume and should be positioned approximately in the centre of a cylindrical cadmium box with 1mm thick wall and a height to diameter ration of 2

ii The nuclide should be the type that obeys HΦgdahl convention

iii The neutron flux should be homogeneous and isotropic, with epithermal flux obeying $\frac{1}{E}$ law down to 0.35eV (where T(E) approaches zero; fig. 2.4)

Thus according to HΦgdahl convention eqn2.11 with the introduction of the concept of E_{cd} split into

$$R = \int_0^{v_{cd}} \sigma(u)\phi(u)du + \int_0^{\infty} \sigma(E)\phi(E)dE \quad \text{.....2.18}$$

Where $V_{cd} = \left[\frac{2E_{cd}}{M_n}\right]^{\frac{1}{2}}$ 2.19

Since $\sigma(u) \sim \frac{1}{v}$ up to V_{cd}, then $\sigma(u) = \sigma_o \frac{v_o}{v}$ where the set σ_o and v_o is chosen arbitrarily. Also since one can assume an undisturbed flux, $\phi_e(E) \sim E^{-(1+\alpha)}$ (or if $\alpha = 0$, $\phi_e(E) \sim E^{-1}$) epithermal spectrum down to E_{cd} in fact down to 0.35eV, we can write for a E^{-1} spectrum

$$\phi(E) = \phi_e(1eV)\frac{1eV}{E} \quad \text{.....2.20}$$

where 1eV is chosen arbitrary as reference energy. If we define the conventional epithermal neutron flux ($cm^{-2}s^{-1}$) as $\phi(E) = \frac{\phi(E)}{E}$, so

$$\int_{E_i}^{E_f} \phi_e(E)dE = \phi_e \int_{E_i}^{E_f} E^{-1}dE = \phi'_e \ln(\frac{E_f}{E_i}) \quad \text{.....2.21}$$

ϕ'_e is known as the true epithermal neutron flux per unit lnE interval. Since from eqn2.21

$$\phi'_e = \frac{\left\{\int_{E_i}^{E_f} \phi_e(E)dE\right\}}{\ln(\frac{E_f}{E_i})} \quad \text{.....2.22}$$

Where E_f and E_i are the high and low boundaries of the epithermal spectrum. But

$\phi(u) = n(v)v$, so equation 2.18 can be written as $R = \sigma_o v_o \int_0^{v_{cd}} n(v)dv + \phi'_e(1eV)\int_{v_{ed}}^{\infty} \frac{\sigma(E)}{E}dE = \sigma_o n_o n_s + \phi'_e I_o = \phi_s \sigma_o + \phi'_e I_o$ 2.23

Where I_o is the resonance integral for E^{-1} spectrum and it is given by

$$I_o = \int_{v_{cd}}^{\infty} \sigma(E)\frac{dE}{E} \quad \text{.....2.24}$$

and n_s is the sub cadmium neutron density (cm^3) given as

$$n_s = \int_o^\infty n(v)dv \quad \text{.....2.25}$$

ϕ_s is the conventional sub cadmium neutron flux ($cm^{-3}s^{-1}$) and it is written as

$$\phi_s = v_o n_s \quad \text{.....2.26}$$

Similarly for $E^{-(1+\alpha)}$ spectrum

$$\phi_e(E) = \frac{\phi_e(1eV)1eV^{1+\alpha}}{E^{1+\alpha}} = \frac{\phi_e' 1eV}{E^{1+\alpha}} \quad \text{.....2.27}$$

$$\phi_e = \frac{\left\{\int_{E_i}^{E_f} \phi_e(E)dE\right\}}{1eV^{\alpha}\left(\frac{-E^{-\alpha}}{\alpha}\right)_{E_i}^{E_f}} \quad \text{.....2.28}$$

Thus

$$\text{R} = \sigma_o v_o \int_0^{v_{cd}} n(u)du + \phi_e' 1eV^{\alpha} \int_{v_{cd}}^{\infty} \sigma(E)\frac{dE}{E^{1+\alpha}} \quad \text{.....2.29}$$

$$= \sigma_0 n_0 n_s + \phi_e' I_0(\alpha) = \phi_s \sigma_o + \phi_e' I_o(\alpha)$$

where $I_o(\alpha)$ is the resonance integral for $E^{-(1+\alpha)} spectrum(cm^2)$ and is given by

$$I_0(\alpha) = 1eV \int_{v_{cd}}^{\infty} \sigma(E) \frac{dE}{E^{1+\alpha}} \quad \text{.....2.30}$$

The relation between I_o and $I_o(\alpha)$ necessitates the introduction of a parameter called effective resonance energy, E_r

When a nuclide is irradiated under a cadmium cover in the aforementioned standard condition, the direct experimental determination of the epicadmium reaction rate, R_e is possible. R_e is described simply as

$R_e = \phi_e' I_o(\alpha)$ or $R_e = \phi_e' I_o$ 2.31

The subcadmium reaction rate R_s written as

$R_s = \phi_s \sigma_o$ 2.32

is the difference between the experimentally determined R and R_e values.

The ratio $\frac{R}{R_e} = \frac{\phi_s \sigma_o + \phi_e' I_o(\alpha)}{\phi_e' I_o(\alpha)} = \frac{f}{Q_o(\alpha)} + 1$ 2.33

Or $\frac{R}{R_e} = \frac{\phi_s \sigma_o + \phi_e' I_o}{\phi_e' I_o} = \frac{f}{Q_o(\alpha)} + 1$ 2.34

Where $f = \frac{\phi_s}{\phi_e'}$ is the ratio of subcadmium to epithermal

$Q_o(\alpha) = \frac{I_o(\alpha)}{\sigma}$ and $Q_o = \frac{I_o}{\sigma}$ ……..2.35

R and R_e cannot be determined simultaneously by irradiating together a bared and cadmium covered nuclide, since cadmium causes significant flux depression in its vicinity (IAEA, 1970).

2.2.1 MECHANISM OF HΦGDHL'S CONVENTION

The mechanism of HΦgdhl convention is as follows

i) The σ_o and I_o values are found for an ultimate cross-sections standard by methods independent of neutron activation (Holden, 1981). The most common standard is $^{197}Au(n,\gamma)^{198}Au$ (De Corte, 1987)

ii) By measuring R_{Au} and $R_{e,Au}$, One can determine ϕ_s, ϕ_e' and f for any irradiation site from eqns2.31, 2.32, 2.33

iii) Finally, applying the same equations, σ_o, I_o and Q_o can be measured from R and R_e measurement for other (n,γ) reaction after converting $I_o(\alpha)$ to I_o

2.2.2 NEUTRON SELF SHIELDING AND CADMIUM TRANSMISSION FACTOR

Some correction factors must be introduced in the equations describing R and R_e in order to correct the reaction rate to the signal obtained from (n, γ) activation. The correction factors are

i) Thermal neutron self shielding factors, G_{th} ($G_{th} \leq 1$). It depends on the nucleus density and on σ_o. The factor has to be multiplied by $\phi_s\sigma_0$

ii) Epithermal neutrons self-shielding factor $G_e (G_e \leq 1)$. It depends on the nucleus density and resonance parameters. Thus, it has to be multiplied by $\phi'_e I_o(\alpha)$ or $\phi'_e I_o$

iii) The cadmium transmission factor for epithermal neutrons (F_{cd}). For most nuclides, F_{cd} is equal to unity, for some, it is less than unity and in exceptional cases, it can be greater than one. It has to be multiplied by $\phi'_e I_o(\alpha)$ or $\phi'_e I_o$, but only when irradiation is done under cadmium cover.

From the above conditions eqns2.29, 2.31, 2.32 and 2.33 should be re- written as

$$R = G_{th}\phi_s\sigma_o + G_e\phi'_e I_o(\alpha) \quad \text{.....2.36}$$

$$R_e = G_e F_{cd}\phi'_e I_o(\alpha) \quad \text{.....2.37}$$

$$R_s = G_{th}\phi_s\sigma_o \text{ (only if } F_{cd} = 1) \quad \text{.....2.38}$$

$$F_{cd}R_{cd} = \left[\frac{G_{th}F}{G_e\phi_o(\alpha)}\right] + 1 \quad \text{.....2.39}$$

And same follows for α = 0

2.2.3 ACTIVATION EQUATION

If we consider an (n, γ) activation with subsequent gamma-spectromety using Germanium detector we can write the relation between the reaction rate and the number of counts (N_p) collected in the full-energy peak as

$$R = \frac{Np/tm}{SDCw} \Big/ \frac{N_A \theta \varepsilon_p \gamma}{m} \quad \text{.....2.40}$$

Or $$R_e = \left[\frac{Np/tm}{SDCW}\right]_{cd} \Big/ \frac{N_A \theta \varepsilon_p \gamma}{m} \quad \text{.....2.41}$$

On the condition that the measured radionuclide is directly formed by (n,γ) reaction is negligible. Where D = decay factor = $e^{-\lambda t_d}$; t_d = decay time , λ = decay constant = $\frac{\ln 2}{T_{\frac{1}{2}}}$, Np = number of counts in the full energy peak, t_m = measuring time, S = Saturation factor $\left[1-\exp(-\lambda t_{irr})\right]$, t_{irr} is the irradiation time

W = mass of the irradiated sample in gram, $\theta = isotopic$ abundance, $\varepsilon_p = full-energy$ peak detection efficiency, $\gamma = absolute$ gamma intensity.

Let the specific activity ($S^{-1}g^{-1}$) be

$$A_{sp} = \frac{Np/tm}{SDCW} \quad \text{.....2.42}$$

Then by substituting eqns2.42 , 2.36 and 2.37 in eqn2.40 and 2.41, we obtain the activation equation in the condition of stable $\phi'_e, \phi_s and \alpha$ during irradiation time t_{irr} as

$$A_{sp} = \frac{N_A \theta \gamma}{m}[G_{th}\phi_s \sigma_o + G_e \phi'_e I_o(\alpha)]\varepsilon_p \quad \text{.....2.43}$$

Or $$A_{sp} = \frac{N_A \theta \gamma}{m} G_e F_e \phi_s I_o(\alpha)\varepsilon_p \quad \text{.....2.44}$$

Then $$A_{sp} - \frac{(A_{sp})_{cd}}{F_{cd}} = \frac{N_A \theta \gamma}{m} G_{th}\sigma_s \sigma_o \varepsilon_p \quad \text{.....2.45}$$

This is the difference between eqns2.43 and 2.44 and it is called cadmium difference, provided the same ε_p value is involved.

Therefore, the experimental measured cadmium ratio, R_{cd} is

$$R_{cd} = \frac{A_{sp}}{(A_{sp})_{cd}} \quad \text{.....2.46}$$

2.2.4 PRINCIPLES OF STANDARDIZATION

Provided the neutron irradiation facility is kept unchanged, the neutron flux will be constant and the induce activity will only be a function of irradiation, decay and measuring time. In the case of irradiation with isotropic neutron sources, only the source strength as a function of time will have to be considered, as the decay time of the source is well known. Consequently the system needs to be standardized once.

In (n,γ) activation analysis, the mass of the element to be determined (i.e. the analyte, index a) in the sample can be obtained from equation 2.43 and 2.44, when the sample is irradiated in the whole neutron spectrum and under cadmium cover (ENAA) yielding respectively.

$$W_a = \frac{M_a \left[\frac{Np/t_m}{SDC} \right]_a}{N_a \theta_a \gamma_a G_{th,a} \phi_s \sigma_{o,a} + G_{e,a} \phi_e I_{o,a}(\alpha) \varepsilon_{p,a}} \quad \text{.....2.47}$$

$$W_a = \frac{M_a \left[(\frac{Np/t_m}{SDC})_{cc} \right]_a}{N_a \theta_a \gamma_a G_{e,a} F_{cd,a} \phi_e I_{o,a}(\alpha) \varepsilon_{p,a}} \quad \text{.....2.48}$$

The actual determination of W_a (concentration of analyte) can be based on various standardization methods employed.

2.2.5 RELATIVE STANDARDIZATION

In relative standardization method, each sample is co-irradiated with a known, mass of the standard element (index, s) to be determined, both are counted in the same geometry with respect to the detector. Thus eqn2.47 and 2.48 could be written as

$$W_a = \frac{\left[\frac{Np/t_m}{DC} \right]_a G_{th,s} f + G_{e,s} Q_{o,s}(\alpha) \varepsilon_{p,s}}{\left[\frac{Np/t_m}{DCW} \right]_{,s} G_{th,a} f + G_{e,a} Q_{o,a}(\alpha) \varepsilon_{p,a}} \quad \text{.....2.49}$$

and

$$W_a = \frac{\left[\frac{Np/t_m}{DC} \right]_{cd,a} G_{e,s} \varepsilon_{p,s}}{\left[\frac{Np/t_m}{DCW} \right]_{cd,s} Ge,a \varepsilon_{p,a}} \quad \text{.....2.50}$$

respectively. Since $S_a = S_s$, $M_a = M_s$, $\gamma_a = \gamma_s$, $\sigma_{0,a} = \sigma_{o,s}, I_{o,a} = I_{0,s}$ and $\theta_a = \theta_s$ in the above equations, it has been assumed that flux gradients between sample and standard location in the irradiation site are negligible.

The factor, f_o can be eliminated if only $G_{e,s}Q_{o,s}(\alpha) << G_{th,S}f$ and $G_{e,a}Q_{o,a}(\alpha) = G_{th,a}f$ Then eqns2.49 and 2.50 may be written as

$$W_a = \frac{\left[\frac{Np/t_m}{DC}\right]_a}{\left[\frac{Np/t_m}{DCW}\right]_s} \quad \text{.....2.51}$$

and

$$W_a = \frac{\left[[\frac{Np/t_m}{DC}]_{cd}\right]_a}{\left[(\frac{Np/t_m}{DCW})_{cd}\right]_s} \quad \text{.....2.52}$$

In terms of concentration, they are written as

$$p_a(ppm) = \frac{\left[\frac{Np/t_m}{DCW}\right]_a}{\left[\frac{Np/t_m}{DCW}\right]_s} \times 10^6 \quad \text{.....2.53}$$

and

$$p_a(ppm) = \frac{\left(\left[\frac{Np/t_m}{DCW}\right]_a\right)_{cd}}{\left(\left[\frac{Np/t_m}{DCW}\right]_s\right)_{cd}} \times 10^6 \quad \ldots\ldots\ldots\ldots\ldots\ldots\ldots\ldots\ldots\ldots\ldots\ldots\ldots\ldots\ldots\ldots 2.54$$

respectively. Where W is the sample mass in gram.

However, the obvious disadvantage of the method is in routine multi-element NAA, where sample preparation, counting and spectral evaluation of the standard is laborious and irksome; especially in the case of unexpected element for which no standard has been co-irradiated.

2.2.6 ABSOLUTE METHOD

If we expressed eqn2.43 for the analyte and a flux monitor (index m) co-irradiated with the sample, the combination yields

$$P_a(ppm) = \frac{A_{sp,a}}{A_{sp,m}} \cdot \frac{M_a \theta_m \gamma_m \sigma_{o,m}}{M_m \theta_a \gamma_a, \sigma_{o,a}} \cdot \frac{G_{th,m} f + G_{em} Q_{o,m} w \varepsilon_{pm}}{G_{th,a} f + G_{e,a} Q_{o,a}(\alpha) \varepsilon_{p,a}} \times 10^6 \quad \ldots\ldots\ldots\ldots 2.55$$

Assuming θ_s, f and α all remain constant during irradiation.

The method, though experimentally very simple can not be considered as practicable as too many uncertainties are introduced because, it require the precise knowledge of the parameters, M, θ, γ, and σ_0 for both analyte and monitor, which may lead to the lost of accuracy of the analytical results.

2.2.7 THE SINGLE COMPARATOR METHOD

Girardi originated this technique (De' Corte, 1970). The NAA single comparator method utilizes the use of so called k-factors, which are experimentally determined by co-irradiation of a sample and a single comparator (mono-standard, index c)

$$K_c(s) = \frac{A_{sp,s}}{A_{sp,c}} \quad \text{.....2.56}$$

From eqn2.43, it means that definition of $K_c(s)$ is

$$K_c(s) = \frac{M_c \theta_s \gamma_s \sigma_{o,s}}{M_s \theta_o \gamma_c \sigma_{o,c}} . \frac{G_{ths} f + G_{e,s} Q_{o,s}(\alpha)}{G_{th,c} f + G_{e,c} Q_{0,c}(\alpha)} . \frac{\varepsilon_{p,s}}{\varepsilon_{p,c}} \quad \text{.....2.57}$$

It then follows that the concentrations of analyte can be obtained from Co-irradiation of sample and single comparator.

$$P_a(ppm) = \frac{A_{sp,a}}{A_{sp,c}} . \frac{1}{K_c(s)} . 10^6 \quad \text{.....2.58}$$

Provided that $\theta_a = \theta_s, G_{th} = G_e = 1, f$ and α show no significant difference in the irradiation condition of analysis and $K_c(s)$ determination, all flux parameters (ϕ_s, f and α) remain constant during irradiation. When properly performed, it has an estimated accuracy of 3% or less. Its obvious advantage in the experimental simplicity; on condition that K- factors are determined a priori; It is useful in routine analysis of long series similar samples (De Corte, 1987). The draw back of the method is that it is bound to local experimental conditions, sometimes with awkward consequence.

2.2.8 THE K_0-STANDARDIZATION

The concept of the NAA k_o-Standardization method was launched in 1975 (De Corte, 1987) and may be approached in two ways.

i). Normalizing the experimentally determined K-Factors of the single comparator for the conditions of irradiation (f,α) and counting(ε_p). one obtains from eq 2.56

$$K_{0,c}(s) = K_c(s).\frac{G_{th,c}f + G_{e,c}Q_{o,c}(\alpha)}{G_{th,s}f + G_{e,c}Q_{0,s}(\alpha)}.\frac{\varepsilon_{p,c}}{\varepsilon_{p,s}} \quad \text{.....2.59}$$

$$\frac{A_{sp,s}}{A_{sp,c}}.\frac{G_{th,c}f + G_{e,c}Q_{o,c}(\alpha)}{G_{e,s}f + G_{e,c}Q_{0,s}(\alpha)}.\frac{\varepsilon_{p,c}}{\varepsilon_{p,s}} \quad \text{.....2.60}$$

From eqn2.46, the $K_{o,c}(s)$ is defined as a composite nuclear constant

$$K_{o,c}(s) = \frac{M_c\theta_s\sigma_{o,s}\gamma_s}{M_s\theta_c\sigma_{0,c}\gamma_c} \quad \text{.....2.61}$$

Supposing that a sample is co-irradiated with a monitor (index) for which an experimentally determined $K_{o,c}(m)$-factor is available (replace s by m in eq 2.60 and definition of eq 2.61). Then, converting $\frac{K_{o,c}(s)}{K_{o,c}(m)} = K_{o,m}(s)$ to the analysis condition of the irradiation (f,α) and counting (ε_p), the analyte concentration can be obtained as [with $K_{o,c}(s) = K_{o,c}(a)$]

$$P_a(ppm) = \frac{A_{sp,a}}{Asp,m}.\frac{K_{o,c}(m)}{K_{o,c}(a)}..\frac{G_{th,m}f + G_{e,m}Q_{o,m}(\alpha)}{G_{th,a}f + G_{e,a}Q_{0,a}(\alpha)}.\frac{\varepsilon_{p,m}}{\varepsilon_{p,a}} \times 10^6 \quad \text{.....2.62}$$

Provided there is no natural isotopic variability ($\theta_a = \theta_c$)

Hence the K_o-method can be interpreted as a single-comparator standardization, which is made completely versatile with respect to both irradiation and counting conditions.

ii) By substituting the nuclear data set in the absolute standardization method of eqn2.55 with one single composite nuclear constant $K_{o,m}(a)$ and one obtains

$$P(ppm) = \frac{A_{sp,a}}{Asp,m} \cdot \frac{1}{K_{o,m}(a)} \cdot \frac{G_{th,m} f + G_{e,m} Q_{o,m}(\alpha)}{G_{th,a} f + G_{e,a} Q_{0,a}(\alpha)} \cdot \frac{\varepsilon_{p,m}}{\varepsilon_{p,a}} \times 10^6 \ldots\ldots\ldots\ldots \quad 2.63$$

Provided flux parameter $(\phi_s, f$ and $\alpha)$ remain constant during irradiation. Based on these, the k_0-method can be interpreted as an absolute standardization with substitution of the nuclear data set for experimentally determined k_0-factors. This eliminates systems errors due to unreliability and uncertainty of nuclear data, On condition that the experimentally determined k_0-factors are accurate. The value of ratio of resonance to thermal neutron cross section, $Q_0(\alpha)$ is given by

$$Q_0(\alpha) = \frac{Q_o - 0.429}{(\overline{E}_r)^{\alpha}} + \frac{0.429}{(2\alpha + 1)(0.55)^{\alpha}} \ldots\ldots\ldots\ldots\ldots\ldots\ldots\ldots\ldots\ldots\ldots\ldots\ldots\ldots 2.64$$

where $\overline{E}_r$ is the effective resonance energy.

2.2.9 GEOLOGY OF BAUXITE

Clay-like sediments composed mainly of alumina and iron-oxide and practically devoid of silica were first described by P. Bethier in 1826 in the vicinity of Le,Baux of the Alpilles (Bouches du Rhone) in south east France (Valeton, 1972). Such sediments were later named "Bauxite" from their type locality. Later, the term was extended to cover lateritic weathering products rich in gibbsite on basalt of the Vogelberg in Germany. The term 'bauxite' refers to a natural material that can be economically processed to high purity alumina in the Bayer process, thus bauxite ore can be defined as bauxite which are economically mineable at present or in the foreseeable future containing 45.50% Al_2O_3 and not more than 20% Fe_2O_3 and 3-5% silicon *IV* Oxide SiO_2 (Valeton, 1972).

Bauxite can be structureless, granular or earthy, Pisolitic and concretionary, massive or stratified, or largely pseudomorphic after the parent rock. The colour ranges from brown, grey to white. Older bauxites that may have been subjected to burial are hard and compact with boehmite and diaaspore commonly being the dominant aluminous minerals. More recent bauxites are generally softer, with gibbsite commonly being the dominant aluminous mineral. The primary constituent is a mixture of Aluminium hydroxides Gibbsite (Al_2O_3 .$3H_2O$) Boehmite (Al_2O_3 .$3H_2O$) and to a lesser content, diaspore (Al_2O_3 .$3H_2O$). Other components are iron oxides, guartz, titanium oxide and elements in minor or trace amount (Shaffer, 1975).

The geographical distribution of bauxite suggests that bauxite deposits can be grouped into large provinces such as the Caribbean province in Central America, the Guayana shield province in South America, the Guinea shield province and Cameroon province in Africa and the Australia province. Smaller province include those of Indonesia and Malaysia, China, South Europe and Arkanas in United States.

Bauxite is found throughout the geological sequence, from Cambria to the Recent. The distribution of bauxite in geological time seems indicate that late Paleozoic, middle to late cretaceous and middle to late tertiary were favourable periods for bauxite formation. The distribution is a result of climatic and tectonic conditions which favored sustained weathering processes leading to the enrichment of Aluminium hydroxides. The conditions may also be characterized by thick terrestrial and paralic formations on shields and self regions, extensive blanket of sandstones and Kaolinite clays, coal deposits, ferralitic soils and sedimentary iron ore.

2.3.0 ECONOMIC IMPORTANCE OF BAUXITE

Early uses of bauxite were recorded in 5300B.C when various bauxite type silicates were being treated in Northern Iraq (Banks, 1979). It is used for making building stones. Some ancient temples and even more recent structure in India have been made from these building stones. They are used as decorative. Bauxite has also been used for road surfacing (Cameron, 1972) but mainly because other materials were not readly available then. Now Aluminium industry consumes about 90% of the total world production of bauxite. It is a major source of raw material for this industry and will continue to be during the foreseeable future (Patternson, 1977). About 10% of the total world bauxite production is consumed by the non-metallurgical industries. It is used mainly in the manufacture of refractory products (Synthetic mullite, high grade alumina fire bricks, castable, monoliths, cements and ramming mixtures used by iron, steel and cement industries), aluminous chemicals and abrasives (Huanganrd Megee, 1988) Chemicals made from bauxite are Alumminium Sulphate (Al_2SO_3), Sodium Aluminate ($NaAlNO_3$) for water treatment, Aluminium chloride

$(AlCl_3)$, for refining crude petroleum. The abrasive products include coated abrasives, sharpening stones and grinding wheels. Other uses are in decolorization and clarification of raw sugar and lubricating oils (Shaffer, 1978).

The refining of bauxite into alumina (High purity Aluminium oxide (Al_2O_3) containing 52.9% Aluminium and 47.1% Oxygen) and its subsequent melting into Aluminium is done via Bayer process. The Bayer process which is the most economical method of refining bauxite takes the advantage of the reaction of trihydroxide or hydroxides of Aluminium with aqueous caustic soda (NaOH) to form Sodium aluminate ($NaAlO_2$).

$AlO(OH) + N_a AlO_2 + H_2O$.

$Al(OH)_3 + N_aOH \rightarrow N_a AlO_2 + 3H_2O$

Aluminium which is the main product formed after electrolysis, which copper and iron top the lost of metals as far as their importance is concerned. Typically, Aluminium has many advantages over other metals due to its low density ($2.7g/cm^3$) high electrical and thermal conductivity and high resistance to corrosion.

In fact Aluminium consumption rate reflects the state of industrialization of a country to a large extent and there is a close relationship between Gross National Product (GNP) and Aluminium consumption (Banks, 1979). The greatest consumers of Aluminium are the developed countries of the world with United States toping the largest consumer, and consumption exceeds expected demand. For instance, the American National Association of Aluminium Distributors (NAAD) members handle about 2.7billion U.S dollars in Aluminium sales every year (Cassidy, 1993). Since the commencement of production and consumption of aluminium, there is always a tremendous increased in both the production and

consumption rate every year. World wide about 15% of the total Aluminium produced every year is consumed in the electrical and communication industries, 11% in house hold equipments, 14% in the manufacture of industrial and agricultural machineries, 11% in containers and packaging material.. Also fairly large amount go to the manufacture of motor. Vehicles, air crafts, irrigation equipments, military supplies, metallurgical and chemical materials (Pennington, 1994).

CHAPTER THREE

3.0 MATERIALS AND METHODOLOGY

3.1.0 Sample Collection: All the raw samples used in this work were collected from Mambilla Plateau, Taraba State. Other samples were obtained from C.E.R.T NAA Lab. The field trip to the Mambilla plateau took place in February, 2008. The following localities were visited; Yelwa, Nguroje and Gembu as Shown in fig3.1.. Samples were collected from pits sunk on the top of the plateau using hand held driven auger and a hammer in the three paces visited.

3.1.1 Brief Geography of the Mambilla Plateau:

Mambilla plateau is located in the north eastern part Nigeria between longitudes 11^{o}E and $11^{o}20'$E, latitude $6^{o}40''$ and $7^{o}20'$ north of the equator. It is about 1800 meter above sea-level with and annual rain fall of 1778mm followed by 2 to 3 months of dry seasons (Bawden and Tule,1966). The Plateau has a maximum length of about 97km (Morgan and Pugh, 1969) and is part of Adamawa mountains notable as the basement exposure at the greatest elevation in West Africa. Major soil types found around the area are eutropic brown soils. (and herentiated) and reddish brown soils (Agboola, 1979). The plateau is noted for its rich scenic beauty and temperate climate with pasture green vegetation. Eroded bedland of the plateau are cut by a ramified course of the River Kam and its numerous tributaries, the final product of which are giant crayon and forbidden mountain crags. A synopsis of the main types of rocks found in the area is given by Ikejiaku (1978) as follows: biotite granite, dolerite, ultramafic roc, pegmatites, quartz veins and basalt with high grade of regional metamorphism affecting basement rock.

3.1.2 Sample Preparation

The raw samples collected were all in lump form. They were crushed with the help of mortar and piston. First the mortar and the piston were brushed thoroughly with an iron brush to remove any solid waste present. They were then washed, rinsed with distil water and dried. Finally, they were rinsed with acetone and air-dried. The first sample was put in the mortar and crushed with piston to powdered solid. The crushing was done manually.

Sieving; the sieve of pore size 150μm was used. The sieve was first brushed, washed with acetone and dried before the sample was poured. The sieve was clamped to a machine which is being operated by electrical power. The sieving was done mechanically.

The above processes were repeated for the remaining two samples and each time, the cleaning processes described above were carried out to avoid contamination. All these were done in Geology Department Laboratory.

The fine powdered samples ($\approx 150\mu m$ in size) were oven dried in Centre for Energy Research and Training (CERT) to remove any moisture present

3.1.3 Sample Preparation for Irradiation using $^{241}Am-Be$ neutron source

The containers for irradiation in this neutron source were plastic vials. The Vials were bought from the market. The containers and their covers were soaked in acidified water for about 24 hours to remove any impurities present and were all air-dried.

Weighing: The weighing of the samples was done using electronic weighing machine(digital balance) available in CERT. The weighing processes were carried out in the following ways:

i) The empty plastic vial was weighed and the mass recorded.

ii) The sample was put in this container and re-weighed.

The mass of the sample in the plastic vial was determined as follows;

iii) Step (ii) - Step (i)

i.e. mass of the vial with sample – mass of the empty vial.

To every sample, a thin film (about 1mm thick) of gold foil was weighed and attached by means of cellotape. The samples were numbered for easy identification. The results are shown in Table4.1. Strings of approximately 1 meter long were tied to each sample. This serve as a means of sending the sample to the irradiation sites of the $^{241}Am-Be$ neutron source and also by it, the sample is retrieve for counting.

3.2.0 Experimental Set-Up

The experimental set-up include $^{241}Am-Be$ neutron source irradiation facility and a $3"\times3"$ $N_aI(Tl)$ detector produced by Cambera Inc. for counting

3.2.1 $^{241}Am-Be$ Neutron Source Irradiation Facility:

The source was manufactured in China and was supplied by the IAEA (International Atomic Energy Agency) under a technical cooperation with CERT ABU Zaria, Nigeria. It is a 5Ci Source with Half-life of 433 Years and Source strength of 1.29 X 10^7 n/s. The source is still about 99% active up till present. The moderating system used in thermalizing this source was cast from commercial paraffin, obtained from Kaduna Refinery and Petrochemical (Onojah, 1995).

In the design, seven polyethylene pipes of 30mm in diameter, one for the source and the remaining six for sample holders were used. The sample holders were each 25mm from the source holder. In between and around these sample holders was a cast of paraffin wax of 750mm in diameter and a height of 600mm with the source at the centre, with a minimum source to source diameter of 250mm to serve as a moderating material for the fast neutrons. The set-up is as shown in fig3.2

The design and construction was made in such a way that the paraffin moderator is co-axial with the cylindrical source while the six irradiation sites were arranged symmetrically round the source. The irradiation tubes are 500mm long with a diameter of 30mm like the source and are all centered on circle through the median plane of the source with a diameter of 80mm. The irradiation facility can take up to 380g powder (Onojah, 1995).

The characterization of this irradiation facility has been carried out with high purity Indium foil used as flux monitors (Onojah, 1995). An extensive characterization of the irradiation facility for use via K_o-INAA method using Indium foils and high purity gold foils as flux monitor was done as well (Rabiu, 2005). It is upon the application of this recent characterization of the irradiation facility that this present work is based. Therefore, the values of thermal epithermal flux ratio, f and epithermal flux shaping factors used in this work were all obtained from this recent characterization.

3.2.2 Sodium Iodide Thallium Activated [NaI(Tl)] Detector.

The most efficient techniques of counting and measuring gamma rays and their energies is through their detection by scintillation detectors or spectrometers of which NaI(Tl) detectors is one of such detectors. When gamma rays (energies) fall on NaI(Tl) crystal, their energy is deposited, this

deposited energy in the crystal is converted to pulses of light. The photo multiplier tube detects these pulses of light, which are amplified by the series of dynodes at a higher potential difference and used to activate a scalar.

The counting set-up used in this work consist of a cambera NaI(Tl) detector, Ortec high voltage bin/preamplifier, a computer system (2048C) having a multi channel analyzer (MCA) card and corresponding software (McbMAESTRO, model no: MACE-002). The detector (model 802-4 is a monoclinic crystal assembly, which includes a $3"\times3"$ $NaI(Tl)$ crystal, a photomultiplier tube, an internal Magnetic light shield and chrome plated Aluminium.

The entire system plugs directly into the cambera tube base (model 2007) which combines the bias network with built in preamplifier. The bias specification for the photomultiplier tube is 800-1000 volts but 950 volts was used through this work.

The Ortec high voltage power supply (model 456) and amplifier (Model 485) are in modular form and fitted into the standard Ortec Bin (model 402A). The Bin contains the low voltage power supply and takes any of the standard nuclear instrumentation models (NIM) for nuclear experiment.

The variable high voltage supply (0 – 2500 volts) supply the 900 – 1000 volts used by the photomultiplier tube to function. The 950 volts used in this work was reached by slowly increasing the valuable voltage Knob.

The preamplifier takes the light from the base of the photomultiplier tube, amplifies them to the desired level and send them to McbMAESTRO Card installed in the computer. The McbMAESTRO (2048C) is a multichannel analyser card containing 2048 channel acquisition memory. An input of 0-8 volts (0.5μs to 30μs) from the shaping amplifier is the only external signal required for the pulse height analysis operation. The software

utilizes the techniques with pull down menu for user-friendly operation. All important parameters are displayed on the monitor along with spectral date. The operation frequently used include, preset time, energy calibration, sample description, data acquisition, storage buffer, roi report and peak search among others. The software calculates and display under the roi report; roi number, energy range, gross counts, net counts with the associated errors, centroid, full width at half maximum (FWHM) etc.

3.3.0 Experimental Procedures

3.3.1 Energy calibration: Gamma spectrometry is mainly with multichannel anlyser and the relation between the obtained pulse height or corresponding channel number versus gamma energy has to be established. Theoretically, this relation should be a linear one. However due to imperfection in the pulse amplification and/or the analogue to digital converter (ADC), this relation is not always perfectly linear. It is therefore better to check the fitting at a regular time intervals e.g before the start of series of measurement. This is done by means of source of high and low energy.

In this work energy calibration done prior to all measurement involve the use of two points sources gamma ray standards. These are ^{137}Cs (661.6keV) and ^{60}Co(1178.2kev) and 1332.5keV) standard point sources. The two standard sources were placed 2cm away from the detector and counted for 300secs. The peak positions were determined with the computer by the knowledge of it profile. On Mcb MAESTRO data acquisition

software, the peak search command allows the computer to search and mark prominent peaks. This is followed by calibration command, after which the computer request for the peak data which when supplied completes the energy calibration.

3.3.2 Absolute Efficiency calibration of 3"×3" NaI(Tl) Detector.

In doing absolute efficiency Calibration, energy calibration was done first. This is because the detection efficiency is a function of energy. The following standard point source radio active nuclides were used to accomplish the task. These are ^{137}Cs, ^{60}Co, ^{54}Mn, ^{24}Mg, and ^{241}Am. The table 3.1 below contains the nuclear data of these nuclides used.

Using the data contain in Table 3.1, the present activities of the radionuclides were calculated using the relation (Mossop, 1968)

$A_t = A_0 e^{-\lambda t}$ ……..3.1

Where A_t is the activity of the source after time, t

A_o is the initial activity

λ is the decay constant given by $\frac{\ln 2}{T_{\frac{1}{2}}}$

t is the decay time

$T_{\frac{1}{2}}$ is the half life of the radionuclide.

The result is presented in Table4.2a

Then each of the standard point sources was placed 2cm from the detector and counts for 300 seconds were obtained. The ROI report for the nuclides obtained from the MCA coupled to the detector is presented in table 4.2b

The counts per second (cps) were determined for each nuclide by dividing the net counts by counting time (300s). The absolute efficiencies of the detector was subsequently calculated using the relation (Knoll, 1989)

$$E_{abs} = \frac{\text{number of pulse recorded}}{\text{number of radiation quanta emitted by the source}}$$

$$= \frac{Activitie\sin cps}{A_t x I_r} x100 \ldots\ldots\ldots\ldots\ldots\ldots\ldots\ldots\ldots\ldots\ldots\ldots 3.2$$

Where I_r is the isotopic abundance otherwise known as the branching ratio of gamma energy.

The calculated values of the absolute efficiencies are presented in Table 4.3.

The values of the absolute efficiencies calculated were plotted against their corresponding gamma energies, an exponential decay curve was obtained (see fig 4.1).

3.3.3 Efficiency calibration for Bulk Sample

Owing to the fact that the samples to be analysed were bulk samples and not point sources, there is the need to make correction for the absolute efficiencies of the point sources calculated above.

In this work, a simple and fast method of efficiency calibration for voluminous sample proposed by Ramose et al (1998) was used to determine the efficiency curve for the bulk sample. The approach involves determining the count rate of a standard point source placed on an empty sample container, then with the source on the container filled with NaCl. and water respectively. Each counting was done for 300secs. The results obtained are presented in Table4.4.

From the data obtained, the transmission coefficient, T(E) and self absorption factor, F(E) through water and NaCl were calculated using the relation

$$T(E) = \frac{I}{I_o} \quad \text{.....3.3}$$

$$F(E) = \frac{T(E) - 1}{\ln T(E)} \quad \text{.....3.4}$$

Where I(subscript s and w) are the intensities detected when a point source is placed in the container of NaCl and water respectively. I_o is the intensity detected when the source is placed on an empty container.

A correction factor, f which depends on energy and apparent density was calculated using the relation.

$$f = \frac{F_s(E)}{F_w(E)} \quad \text{.....3.5}$$

The correction factor, f was multiplied by the efficiency of the point source in order to obtained the efficiency of the bulk sample. These values are presented in Table 4.5.

The corrected values of the absolute efficiency were plotted against their corresponding energies to obtain the absolute efficiency curve for the bulk sample (see fig 4.2)

3.3.4 Measurement of Detection limit (L_D) and Detectable mass (M_D)

The isotopic neutron source used in this work has a low neutron flux. It therefore becomes important to measure and calculate the limit of measurement of the elements which are to be determined. By definition, Detection Limit is the limit at which a given analytical procedures may be relied upon to lead to detection. It also refers to the maximum upper limit of the measurement processes.

These limits were measured and calculated for Aluminium and Silicon in this work using the curies method (99.865% confidence limit) corresponding to K = 3 via the equation (Onojah, 1995)

$$L_D = K^2 + 2k(\frac{R_B}{D_t})^{\frac{1}{2}} \quad \text{.....3.6}$$

Where K is the abscissa of the standardized normal distribution, D_t is the counting time and R_B is the background count rates.

The samples used here were Al_2O_3 and SiO_2 from Chemistry Department. They were each weighed, irradiated and counted on the $3" x 3"$ NaI(Tl) detector. The regime is shown Table3.2.

The peak area was marked and the background count-rate and detection limits were determined. The minimum detectable mass was calculated by dividing the detection limits, L_D by the specific activities. The results obtained are presented in Table 4.6.

3.3.5 Sample Irradiation and Counting

The irradiation of the samples was carried out in the paraffin moderating system designed for INS activation analysis (Onojah, 1995). The irradiation was done for Aluminium and silicon from bauxite ores using K_o-NAA approach. The ore samples were co-irradiated with gold foil in the irradiation sites of $^{241}Am-Be$ isotopic neutron source.

From the theory of neutron activation analysis (NAA), the saturation factors of the radio- isotope under analysis is given by

$$S = 1 - e^{-\lambda t_{irr}} \quad \text{.....3.7}$$

Where λ is the decay constant = $\frac{\ln 2}{T_{\frac{1}{2}}}$

t_{irr} is the irradiation time

$T_{\frac{1}{2}}$ is the half-life

Also the decay factor D is given by

$$D = e^{-\lambda t_d} \quad \text{.....3.8}$$

Where t_d is the decay time.

The counting factor, C is given by

$$C = \frac{1 - e^{-\lambda t_m}}{\lambda t_m} \quad \ldots\ldots 3.9$$

Where t_m is the measuring or counting time.

Bearing the above factors (which depend mostly on $T_{\frac{1}{2}}$) in mind, the following regime was used for irradiation and counting of the samples and the attached foil in this work. The results of the counting are presented in table4.7.

All the samples and the foils were allow to decay for a month after which the samples with the attached foils were put in cadmium container and irradiated, delayed and counted for according to the regime in Table3.3. The cadmium containers were used to cut-off the thermal neutrons so that only fast neutron activate the samples. This is because $^{28}Si(n,p)^{28}Al$ is favoured by fast neutron reaction. The results are presented in Table 4.8.

The net counts in Table 4.8 were subtracted from the corresponding one in Table 4.7 to get the actual counts for $^{27}Al(n,\gamma)^{28}Al$ reaction as the former contains counts for both Aluminium and Silicon. The result is shown in Table 4.9. Parts of the raw samples were also sent for Reactor Nuclear Activation Analysis (RNAA) for comparison of results. The result is shown in Table4.10.

Samples of bauxites, bentonites, clayball, felsper, kaolin and three different standards obtained from the N. A. A Laboratory of C.E.R.T. were prepared, irradiated (bare and Cd-cover) and counted for using the regime in Table 3.3. the results of bare and Cd—cover irradiations are shown in Tables4.11 and 4.12 respectively. The peak counts for ^{27}Al(n,γ)^{28}Al is shown in Table4.13.

3.3.6 Determination of Aluminium concentration in the samples via ko-NAA:

The counts per second (cps) of Table4.9 are done. The saturation factor {f), the delay factor(d) and the counting factor(c)and the specific activity(Asp) were calculated for the samples and the foils. The results are presented in Table4.14. Table4.15 contains the nuclear data used while Tabl4.16 contains values of flux shaping parameters and flux ratio, f of the six irradiation sites of the Am-Be neutron source facility use in this work. the data in Tables4.14, 4.15 and 4.16 are used to calculate the Aluminium concentration in part per million (ppm) using the equations 2.63 and 2.64. The result is presented in Table4.17

The procedures above were repeated for Table4.13 and the results are presented in Tables4.18 and 4.19.

3.3.7 Determination of Silicon concentration

The ko-NAA is only suitable for (n,γ) reaction (De-Corte, 1987) and ^{28}Si(n,p)^{28}Al is an (n,p) reaction, therefore we use the Al/Si weight ratio proposed by Jonah, et al (2004)

$$\frac{W_{Al}}{W_{Si}} = \frac{(Np)_{Al}.M_{Al}\theta_{Si} < \sigma_{n,p} > \phi_f}{(Np)_{Si} M_{Si} \theta_{Al} \sigma_{n,\gamma} \phi_s} \quad \text{.....3.10}$$

Or

$$\frac{W_{Al}}{W_{Si}} = K \frac{(Np)_{Al} \phi_f}{(Np)_{Si} \phi_s} \quad \text{.....3.11}$$

Where K= $\frac{M_{Al}\theta_{Si} < \sigma_{n,p} >}{M_{Si}\theta_{Al}\sigma_{n,\gamma}}$ 3.12

Or

$$K = \frac{W_{Al}(Np)_{Si}\phi_s}{W_{Si}(Np)_{Al}\phi_f} \quad \ldots\ldots\ldots\ldots\ldots\ldots\ldots\ldots 3.14$$

Where W_{Al} = weight of Al in the sample

W_{Si} = weight of Si in the sample

Np = the counts

Øs = thermal neutron flux in the irradiation used

$Ø_f$ = fast neutron flux in the irradiation site used

M_{Al} = atomic mass of Aluminium

M_{Si} = atomic mass of silicon

θ_{Si} = lsotopic abundance of silicon

θ_{Al} = lsotopic abundance of silicon

$\sigma n, r$ = thermal neutron cross section

$<\sigma n, p>$= the Am-Be spectrum average cross-section for (n,p) reaction.

K was determined using two different mixtures of high purity Al_2O_3 and SiO_2 in ratio 3:2 and 2:3 by percentage respectively. Each of the mixture was irradiated bare and under Cd-cover in the six irradiation sites of the Am-Be neutron source. A regime of 10minutes irradiation time, 1minute decay time and 10minutes counting time was maintained. The peak counts obtained were presented in Table4.20. The W_{Al}/W_{Si} ratio in 3:2 by percentage of $Al_2O_3 + SiO_2$ is 1.70 while the W_{Al}/W_{Si} in 2:3 by percentage is 0.755. The neutron flux distribution of the six irradiation sites is shown in Table4.21. K-values were calculated from the data available in Tables4.20 and 4.21 using equation3.4 and the results are shown in Table4.22. The average K-value was calculated to be 0.28±0.03. The K-value was also calculated using nuclear constants. M_{Al}=26.98g, M_{Si}=28.09g, θ_{Si}=0.9223, θ_{Al}=1, $\sigma_{n,\gamma}$=252mb and $<\sigma n, p>$=64mb via equation23.3 to be o.24. These two values of K (K_{exp} and K_{eall}) where used to calculate the concentration of Silicon through out this work.

These two values (k_{exp} and k_{call}) the peak counts in tables 4.8, 4.9, the aluminum concentration in table4.17 and the neutron flux distribution of table 4.21 were used to calculate the silicon concentration and Al/Si concentration ratios of the raw samples. The results are presented in Table 4.23. Also using these two values of k (k_{exp} and k_{call}), the peak counts in table 4.12, 4.13, the aluminum concentration in table 4.19 and the neutron flux distribution of the six irradiation site in table 4.21 we calculate the silicon concentrations and Al/Si concentration ratios in other samples. The results are presented in Table 4.24.

Table 3.1: Nuclear data of some radio nuclides

Radio Nuclide	$T_{\frac{1}{2}}(yrs)$	$E_{\gamma}(Kev)$	Isotopic abundances	Date of manufacture	Initial Activities (KBq)
^{137}Cs	30.14	661.6	0.851	14-07-2004	36.9
^{60}Co	5.27	1173.2	0.99	14-07-2004	38.4
^{60}Co	5.27	13332.5	1.00	14-07-2004	38.4
^{57}Co	0.7447	122.1	0.856	14-07-2004	37.7
^{54}Mn	0.856	834.8	1.00	14-07-2004	38.7
$^{22}N_a$	2.6	511.0	1.80	15-07-2004	36.9
$^{22}N_a$	2.6	1274.5	0.999	15-07-2004	36.9
^{24}Am	432.2	59.5	0.359	15-07-2004	36.5

Table 3.2: Irradiation regime for the sample used for measuring Detection limit and Detectable mass

Isotope	Mass	t_{irr}	t_{delay}	t_m
^{27}Al	0.357	1hour	1min	10min
^{28}Si	0.297	1hour	1min	10min

Table 3.3 regime for irradiation, delay and counting for the samples and the foils

Sample	t_{irr}	t_d-sample	t_d-foil	t_m
Ia	1 hour	1min	13min	10min
Ib	1hour	1min	13min	10min

Ic	1hour	1min	13min	10min
Id	1hour	1min	13min	10min
IIa	1hour	1min	13min	10min
IIb	1hour	1min	13min	10min
IIc	1hour	1min	13min	10min
IId	1hour	1min	13min	10min
IIIa	1hour	1min	13min	10min
IIIb	1hour	1min	13min	10min
IIIc	1hour	1min	13min	10min
IIId	1hour	1min	13min	10mi

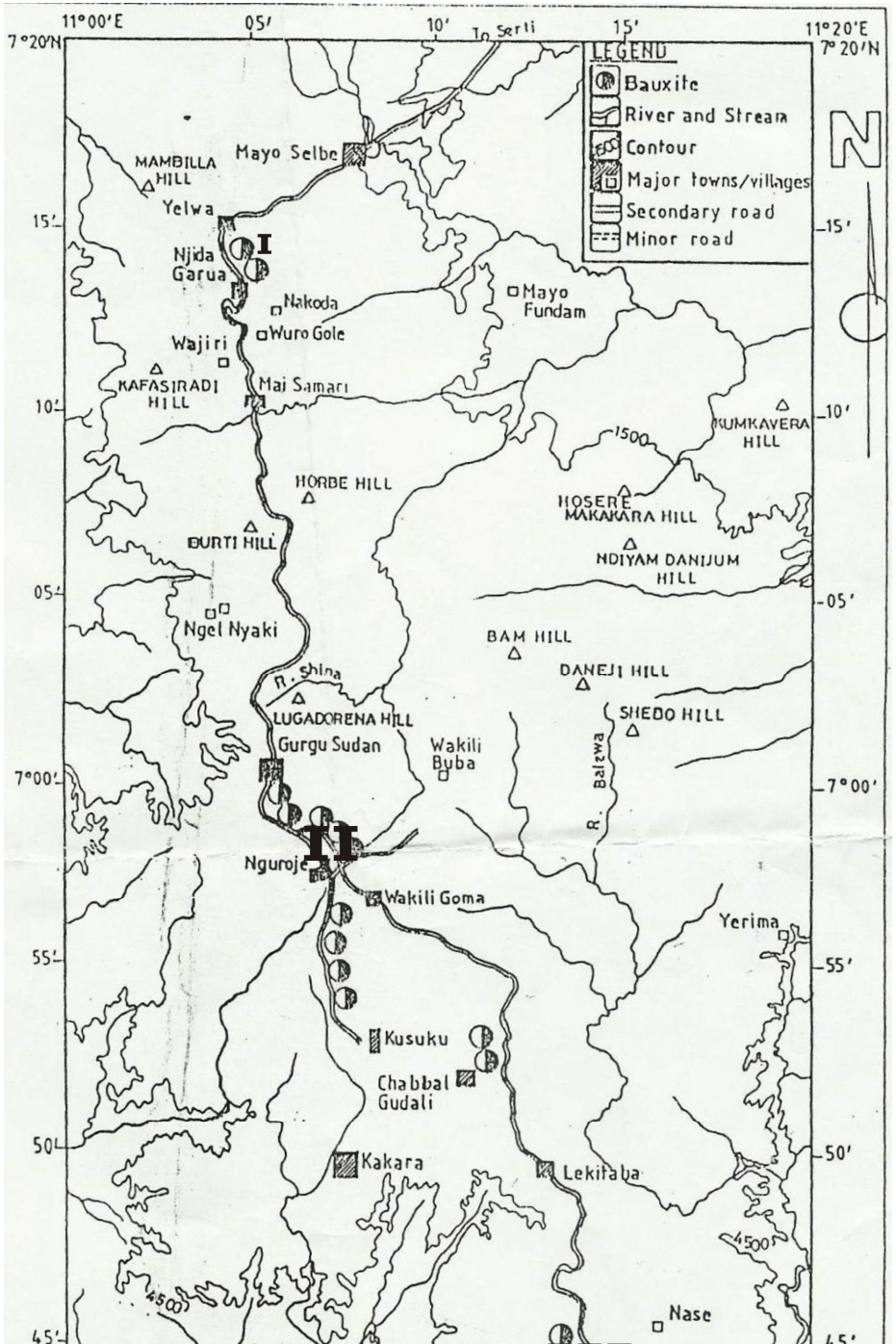

11°00'E
05'
10'
15'
11°20'E
7°20'N
LEGEND
Bauxite
River and Stream
Contour
Major towns/villages
Secondary road
Minor road
N
MAMBILLA HILL
Mayo Selbe
Yelwa
Njida Garua
I
Nakoda
Wuro Gole
Mayo Fundam
Wajiri
KAFASIRADI HILL
Mai Samari
KUMKAVERA HILL
1500
HORBE HILL
HOSERE MAKAKARA HILL
BURTI HILL
NDIYAM DANIJUM HILL
Ngel Nyaki
BAM HILL
DANEJI HILL
R. Shina
LUGADORENA HILL
SHEDO HILL
Gurgu Sudan
Wakili Buba
R. Baltwa
II
Nguroje
Wakili Goma
Yerima
Kusuku
Chabbal Gudali
Kakara
Lekitaba
4500
Nase
15'
10'
05'
7°00'
55'
50'
45'

Fig 3.1: Map of the area where the sample are collected

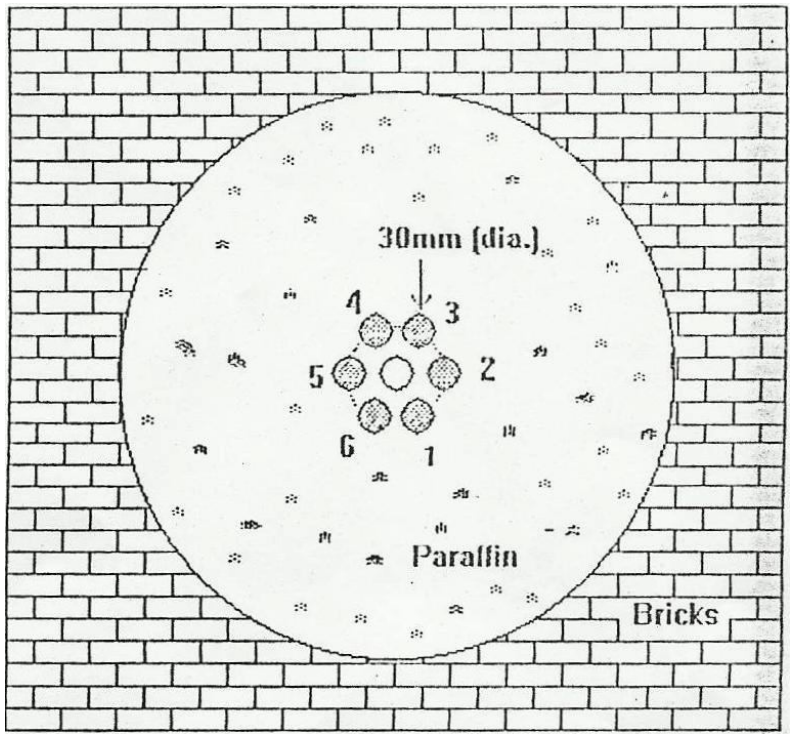


Fig3.2: Illustration of Am-Be set-up in C.E.R.T, A.B.U, Zaria

CHAPTER FOUR

4.0 RESULTS AND DISCUSSIONS

4.1 RESULTS OF CALIBRATIONS

4.1.1 Energy calibration: As explained in chapter three that the relation between the obtained pulse height or corresponding channel number with gamma energy has to be established to be a linear one for any effective gamma ray spectrometry. For this reason the NaI(Tl) detector used in this work for gamma ray spectrometry was calibrated using the standard gamma- ray point sources mentioned in chapter three. This is always done before any set of measurements.

4.1.2 Efficiency calibration: The data in Tables (4.2a and 4.2b) were used to obtain Table 4.3 using equation3.2. The sources were each placed 2cm away from the detector and counted because that is the counting geometry to be used for the samples owing to the short half life (2.24minutes) of the radio-nuclide (^{28}Al) formed. Also counting geometry affects the efficiency of a detector in gamma-ray spectrometry (Ramose et al,1998). The calculated values of absolute efficiencies were used to obtained absolute efficiency curve shown in fig 4.1. The curve shows an exponential decay relation meaning that at very high energies, the absolute efficiencies are low and vice versa.

Since standard point gamma ray sources were used, the efficiency curve presented in fig 4.1 can only be used for point sources and those sources with negligible self absorption coefficient (i.e sources that are very thin). The samples to be analyzed in this work are bulk samples and an accurate determination of the photo peak efficiency of such samples is one of the main problems in gamma ray spectrometry (Ramose et al, 1998). Therefore, there is the need for correction and the approach to this was described in chapter three section 3.4.3

The self absorption factor, F(E) and the transmission coefficient, T(E) of water and sodium chloride (NaCl) were calculated using equations 3.4 and 3.3 respectively. The correction factor, f which depends on apparent density and energy was determined using equation 3.5. The correction factor was multiplied by the efficiency of the point sources (Table4.3) and the result is presented Table4.5.

The corrected values of absolute efficiencies were plotted against their corresponding energies to obtain the absolute efficiency curve for the bulk sample shown in Fig4.2. The curve also shows an exponential decay relation. From this efficiency versus energy curve, one observes the efficiency range of 0 - 27% as against 0 – 29% range for point sources.

We used water because through water, the correction factor, f will only depends on the energy of the sources. Also we used common salt because the densities of the elements of interest are close to the apparent density of the common salt.

4.2 Limit of Detection (L_D) and Detectable Mass (M_D).

Since the neutron source used in this work has low neutron flux, it is important to know these limits for elements to be analyzed. We measured and calculated these limits for Aluminium and Silicon using equation 3.6 and the results are shown in Table4.6.

The results show that the detection of the two elements is possible using the facility but it is easier to detect silicon than aluminium. This is probably due to the large presence of fast neutrons than thermal neutrons in each of the six irradiation sites of the neutron source facility (Rabiu, 2005).

The result also shows that the analytical procedures leading to the detection of the two elements under our consideration is reliable.

4.3 Determination of Aluminium concentration in the samples.

The peak analysis of $^{27}Al(n,\gamma)^{28}Al$ reaction used in the determination of aluminium concentrations in the raw and other samples are shown in the Tables (4.7-4.19). Table4.7 contains the peak counts obtained when the samples and the foils were irradiated bare while Table4.8 contains the peak counts obtained when the samples and the foils were irradiated under Cd-cover. The peak counts in Table4.8 were subtracted from the corresponding peak counts in Table4.7 to obtain the peak counts in Table4.9. This is because during bare irradiation the sample is being activated by both thermal and fast neutrons while irradiation under Cd-cover, the sample is being activated by only fast neutrons as the thermal neutrons are cut-off by the cadmium container. Similarly, the peak counts in Table4.12 were subtracted from the corresponding peak counts in Table4.11 to get the peak counts in Table4.13. The processes leading to Tables (4.14 – 4.25) have been explained in chapter three. When we compare the results of Reactor Neutron Activation Analysis (RNAA) to that of k_o-NAA (Table4.10), there is close agreement within the limit of experimental error. The k_o-NAA results shown in Table4.10 are the average results for a particular sample in Table4.17. The variation in the results of Table4.17 for a particular sample is due to non-uniformity in flux distribution across the six irradiation sites of the Am-Be source. Also the flux shaping parameter α is not the same for the six irradiation sites of the neutron source (Rabiu, 2005).

4.4 Determination of Silicon concentration in samples

As explained earlier $^{28}Si(n,p)^{28}Al$ is an (n,p) nuclear reaction, therefore k_o-NAA is not suitable for its analysis. We used Al/Si weight ratio method (Jonah, et al, 2004) via equations 3.10 to 3.14. Where the Al/Si weight ratios in those equations were replaced with Al/Si concentration ratios. The

average K-value determined experimentally is 0.28 ± 0.03 while the calculated value of K using nuclear constants is 0.24. There is close agreement in these two values of K. The slight dispersion might be from the low counting efficiency. The K_{exp} determined in this work is also in close agreement with the one determined by Jonah et al, 2004 (0.26 ± 0.08). Comparing the ratios in Table4.25, one observes a close agreement in the two results.

Table 4.1: Weighing of samples and the attached foils

Sample no	Mass of empty Vial (g)	Mass of sample + vial (g)	Mass of sample (g)	Mass of foil attached (g)
Ia	0.3300	4.330	4.0	0.0789
Ib	0.3001	4.3001	4.0	0.0786
Ic	0.3002	4.3002	4.0	0.0790
Id	0.3001	4.3001	4.0	0.0787
IIa	0.3001	4.3001	4.0	0.0790
IIb	0.3001	4.3001	4.0	0.0788
IIc	0.3002	4.3002	4.0	0.0790
IId	0.3001	4.3001	4.0	0.0790
IIIa	0.3001	4.3001	4.0	0.0788
IIIb	0.3000	4.3000	4.0	0.0789
IIIc	0.3001	4.3001	4.0	0.0789
IIId	0.3000	4.300	4.0	0.0788

Table 4.2a: the initial activities(A_0) and the final activities(A_t) of the various radio-nuclides

Radio Nuclide	Manufacturing date	Half-life (years)	A_o (KBq)	A_t (KBq)
Cs – ^{137}	14-07-2004	30.14	36.9	33.87
Co – ^{60}	14-07-2004	5.27	38.4	23.51
Co – ^{57}	14-07-2004	0.7447	37.7	1.171
Mn – ^{54}	14-07-2004	0.856	38.7	1.89
Ma – ^{24}	15-07-2004	2.6	36.9	13.65
Am -^{241}	15-07-2004	432.2	36.5	36.28

A_t is the activity of the source calculated on the 8 of April, 2008

Table4.2b: ROI report of the radio-nuclide when placed 2cm away from the detector and counted for 300secs.

LT: 300secs, ACQ 08 APRIL,08

ROI	Range (KeV)	Gross	Net
1-^{137} Cs	555.02 - 721.00	441304	408792±946
2-^{60} Co	1045.97 - 1204.94	227808	141466±1174
3-^{60} Co	1243.40 - 1391.90	177608	126954±895
4-^{57} Co	69.32 – 130.47	69515	44525±411
5-^{54} Mn	736.73 - 907.95	26084	22850± 270
6-^{22} Na	390.74 - 555.02	479089	404846±1227
7-^{22} Na	1182.55-1332.50	99492	80396±626
8-^{241} Am	55.34-130.97	1147931	1128835±1675

Table4.3: Calculated values of the absolute efficiencies of point source.

Radio nuclide	Eγ (KeV)	$T_{1/2}$ (years)	Isotopic abundance	A_t (KBq)	Source activity (cps)	E_{ff} (%)
^{137}Cs	661.6	31.4	0.851	33.87	1362.64±3.15	4.73
^{60}Co	1173.2	5.27	0.99	23.51	471.55± 3.91	2.03
^{60}Co	1332.5	5.27	1.00	23.51	423.18 ±2.98	1.80
^{57}Co	122.1	0.7447	0.856	1.171	148.42±1.37	14.81
^{54}Mn	634.8	0.856	1.00	1.89	76.17±0.90	4.03
^{22}Na	511.0	2.6	1.80	13.65	1349.49 ±4.09	5.49
^{22}Na	1274.5	2.6	0.999	13.65	267.99±2.09	1.97
^{241}Am	59.5	432.2	0.359	36.28	3762.98±5.58	28.89

Table4.4: Peak counts of the point sources in empty container, inside common salt and inside water.

Radio Nuclide	Source activity in empty Container (CPS)	Source activity in NaCI (CPS)	Source activity in Water (CPS)
^{241}Am	37628±3.58	2308.1±2.3	2685122.2±2.5
^{22}Na	1349.5±4.1	917.9±0.8	1103.5±1.9
^{22}Na	268±2.1	182.3±1.1	219.1±2.6
^{54}Mn	76.2±0.9	52.1±2.8	55±2.8
^{60}Co	471.6±3.9	323.2±2.2	340.8±1.6
^{60}Co	423.18±3	289.8±0.3	305.4±1.2
^{57}Co	4715.1±1.4	100.3±1.8	105.8±3.2
^{137}Cs	1362.6±3.2	933±0.5	984.8±3.3

Table4.5: Calculated values of the Transmission coefficients, T(E) Self absorption parameter,F(E) Correction factor, F and the Efficiencies of bulk sample, FE_{ff}.

Radio-nuclide	E_γ (KeV)	T_s (E)	T_w (E)	F_s (E)	F_w (E)	F	E_{ff} (%)	FE_{ff} (%)
^{241}Am	59.5	0.6134	0.7136	0.7910	0.8488	0.9319	28.89	26.92
^{22}Na	511.0	0.6802	0.8177	0.8299	0.9058	0.9162	5.49	5.03
^{22}Na	1278.8	0.6801	0.8176	0.8298	0.9057	0.9162	1.97	1.80
^{54}Mn	834.8	0.6845	0.7217	0.8323	0.8536	0.9750	4.03	3.93
^{60}Co	1173.2	0.6853	0.7227	0.8328	0.8539	0.9753	14.81	14.44
^{60}Co	1332.5	0.6848	0.7228	0.8325	0.9539	0.9749	2.03	1.98
^{57}Co	122.1	0.6757	0.7127	0.8273	0.8483	0.9752	1.80	1.75
^{137}Cs	661.6	0.6853	0.7227	0.8328	0.8539	0.9753	4.73	4.61

Table4.6: Results of measurement of Limit of Detection(L_D) and Detectable Mass(M_D)

Isotope	Mass (g)	$T_{1/2}$	S	D	C	Net count	Background count rate	A_{sp} (cps/g)	L_D (g)	M_D
^{27}Al	0.357	2.24	1	0.734	0.31	6.1				
^{28}Si	0.297	2.24	1	0.734	0.31	78.8				

Table 4.7: Peak counts of bare irradiation of raw samples and foils

Sample no	Irrad site	T_{irr}	t_{delay} sample	t_m	Net counts sample	t_{delay} foil	t_m	Net counts foil
Ia	3	1hour	1min	10min	1701±633	13min	10min	10410±590
Ib	4	»	»	»	16827±623	»	»	9450± 706
Ic	5	»	»	»	17420±607	»	»	10650± 810
Id	6	»	»	»	18120±908	»	»	11676±920
IIa	1	»	»	»	12774±450	»	»	11820±620
IIb	5	»	»	»	12231±400	»	»	9966±890
IIc	2	»	»	»	12470±390	»	»	11190±960

IId	3	»	»	»	12180±300	»	»	10362±760
IIIa	4	»	»	»	3488±250	»	»	11172±770
IIIb	3	»	»	»	3535±202	»	»	9966±999
IIIc	6	»	»	»	3359±240	»	»	9640±801
IIId	5	»	»	»	3640±210	»	»	9882±609 .

Table 4.8: Peak counts of Cd-cover irradiation of raw samples and foils.

Sample no	Irrad Site	t_{irr}	t_{delay} sample	t_m sample	Net counts sample	t_{delay} foil	t_m foil	Net counts foil
Ia	3	1hour	1min	10min	3360±560	13min	10min	10412±580
Ib	4	»	»	»	3174±580	»	»	9460±420
Ic	5	»	»	»	3282±591	»	»	10770±470
Id	6	»	»	»	3296±530	»	»	11800±501
IIa	1	»	»	»	2166±480	»	»	11850±490
IIb	5	»	»	»	2181±360	»	»	10011±512
IIc	2	»	»	»	2072±590	»	»	11200±443
IId	3	»	»	»	1998±216	»	»	10450±457
IIIa	4	»	»	»	3460±258	»	»	11160±510
IIIb	3	»	»	»	3502±241	»	»	9990±488
IIIc	6	»	»	»	3337±230	»	»	11650±499
IIId	5	»	»	»	3607±222	»	»	9900±457

Table 4.9: The real counts for $^{27}\mathrm{Al}(\mathrm{n},\gamma)^{28}\mathrm{Al}$ of raw samples

Sample No	T_{irr}	t_{delay} sample	t_m	Net counts sample	t_{delay} foil	Net counts foil
Ia	1hour	1mins	10mins	14040±847	13mins	10410±690
Ib	»	»	»	13656±851	»	9450±706
Ic	»	»	»	14136±847	»	10650±810
Id	»	»	»	14826±1051	»	11676±920
IIa	»	»	»	10608±657	»	11820±620
IIb	»	»	»	10050±538	»	9966±890
IIc	»	»	»	10398±707	»	11990±960
IId	»	»	»	10122±366	»	10362±760
IIIa	»	»	»	28±5	»	11172±770
IIIb	»	»	»	33±6	»	9966±999
IIIc	»	»	»	22±7	»	11640±801
IIId	»	»	»	33±5	»	9882±609

Table 4.10: Comparism of the Aluminium Concentration obtained from RNAA and k_o-NAA for the raw samples in part per million (ppm)

Sample	I	II	III
RNAA result	115000±8000	83000±6000	BLD
K_0-NAA result	111274±11463	80874±7538	207±68

Table 4.11: Peak counts of bare irradiation of other samples.

Sample	Irrad site	peak counts for bare samples	foil
Bauxite1	4	93±15	11538±690
Bauxite2	3	107±12	11412±706
Bauxite3	1	112±14	11178±810
Bauxite4	2	99±14	11304±820
Bauxite5	5	167±14	11214±710

Bentonite1	6	197±14	10992±887
Bentonite2	3	178±12	11466±800
Bentonite3	4	190±18	11580±687
Bentonite4	2	207±14	11442±730
Clayball	1	228±15	11280±675
Feldspar	5	256±13	11352±800
Kaolin	6	104±17	11532±710
S_1	3	140±15	11532±670
S_2	4	137±16	11418±689
S_3	2	96±14	11280±620 .

S_1 =60%Al_2O_3 +40% SiO_2

S_2 =40%Al_2O_3+60% SiO_2

S_3=BCS-CRM 348.

Table4.12: Peak counts of Cd-cover irradiation of other samples

Sample	Irrad site	peak counts	peak counts for foils
Bauxite1	4	55 ±15	11538±690
Bauxite2	3	60 ±15	11412±706
Bauxite3	1	60±16	11178±810
Bauxite4	2	57±13	11304±820
Bauxite5	5	49±15	11214±710
Bentonite1	6	128±13	10992±887
Bentonite2	3	116 ±16	11466±800
Bentonite3	4	123 ±17	11580±687
Bentonite4	2	122 ±12	11442±730
Clayball	1	130±18	11280±675
Feldspar	5	176±16	11352±800
Kaolin	6	76 ±12	11532±710

S_1	3	57±16	11532±670
S_2	4	77±15	11418±689
S_3	2	61±17	11280±620 .

S_1 =60%Al_2O_3 +40% SiO_2

S_2 =40%Al_2O_3+60% SiO_2

S_3=BCS-CRM 348.

Table 4.13: The peak counts of $^{27}Al(n,\gamma)^{28}Al$ of other samples.

Sample	Irrad site	peak counts for sample	peak counts for Foil .
Bauxite1	4	38± 8	11538±690
Bauxite2	3	47±7	11412±706
Bauxite3	1	52±8	11178±810
Bauxite5	5	58±8	11214±710
Bentonite1	6	69±7	10992±887
Bentonite2	3	62±7	11466±800
Bentonite3	4	67±9	11580±687
Bentonite4	2	85±6	11442±730
Clayball	1	98±8	11280±675
Feldspar	5	80±7	11352±800
Kaolin	6	28±7	11532±710
S_1	3	83±8	11532±670
S_2	4	60±8	11418±689
S_3	2	35±8	11280±620 .

Bauxite4 2 42±7 11304±820

S_1 =60%Al_2O_3 +40% SiO_2

S_2=40%Al_2O_3+60% SiO_2

S_3=BCS-CRM 348.

able4.25: Comparison of results of other samples.

	W_{Al} / W_{Si}(Jonah et al, 2004)		Present work	
Sample	Calculated	Experimental	Calculated	Experiment
Bauxite1	0.71	0.77±0.22	0.62±0.05	0.72±0.05
» 2	0.78	0.84±0.21	0.84±0.02	0.98±0.14
» 3	0.85	0.92±0.23	0.83±0.05	0.97±0.12
» 4	0.73	0.79±0.19	0.6±0.03	0.70±0.11
» 5	1.16	1.25±0.38	0.84±0.22	0.98±0.14
Bentonite1	0.55	0.57±0.07	0.51±0.05	0.59±0.03
» 2	0.54	0.58±0.09	0.57±0.04	0.67±0.08
» 3	0.53	0.57±0.09	0.49±0.05	0.57±0.08
» 4	0.68	074±0.08	0.57±0.08	0.67±0.07
Clayball	0.74	0.80±0.11	0.72±0.04	0.84±0.05
Feldspar	0.42	0.45±0.04	0.32±0.04	0.38±0.07
Kaolin	0.36	0.39±0.08	0.35±0.02	0.41±0.01
40%Al_2O_3+ 60%SiO_2	0.77	0.83±0.19	0.70±0.09	0.81±0.05
60%$Al_2O_{2_3}$ + 40%SiO_2	1.43	1.55±0.43	1.56±0.02	1.30±0.25
Bc-CRM348	0.72	0.78±0.24	0.47±0.29	0.55±0.27

i

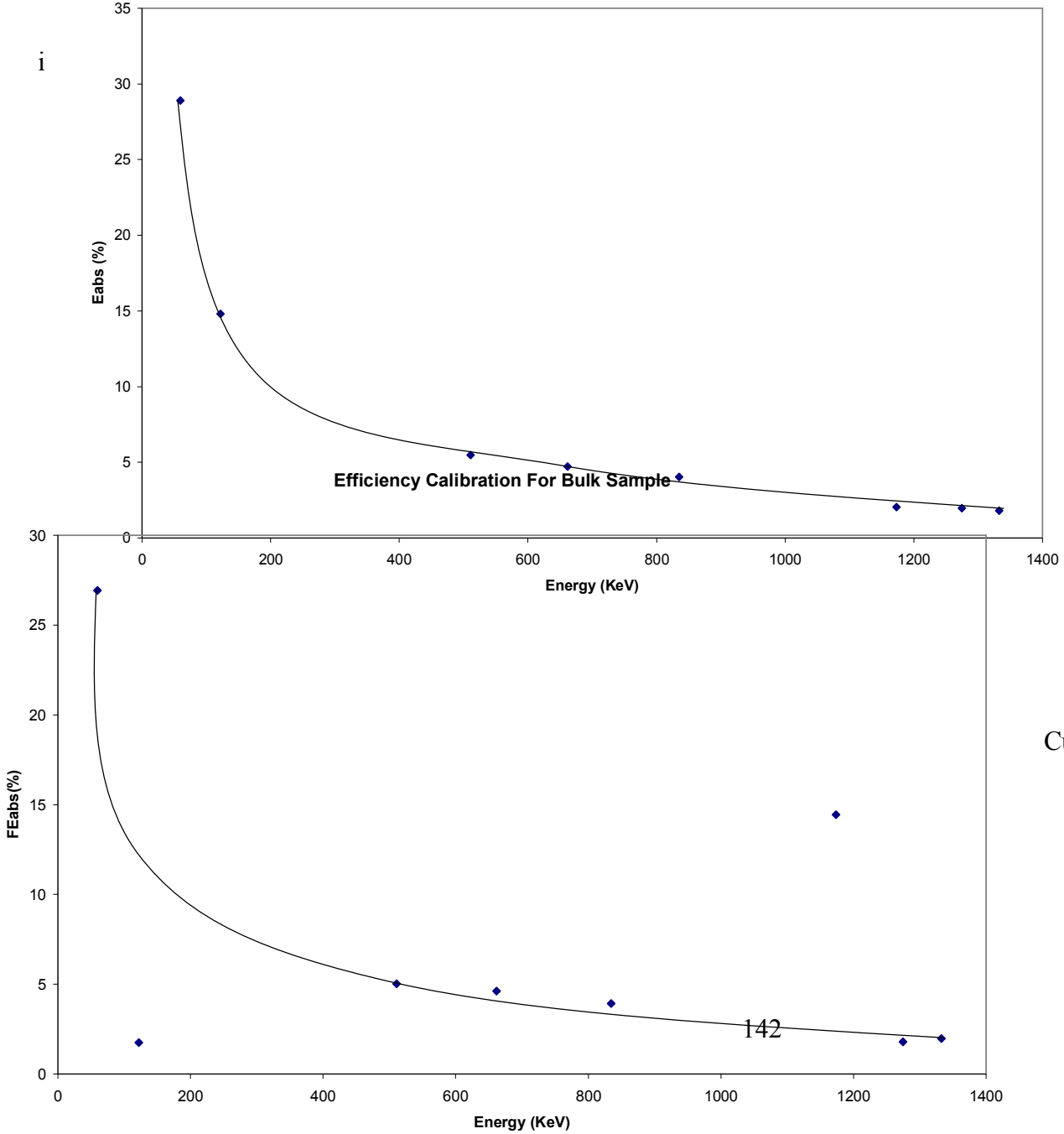


Fig.1: Efficiency Calibration Curve of Point Sources

CHAPTER FIVE

5.0 SUMMARY, CONCLUSION AND RECOMMENDATION.

5.1 SUMMARY.

Chapter one discussed the general introduction of Neutron Activation Analysis (NAA) Techniques and ko-Neutron Activation Analysis (ko-NAA) method. The review of previous works, motivation of the work as well as aims and objectives of the work were all discussed in chapter one.

Chapter two review some related Literatures under the following sub-headings; neutron interactions with matter, classification of neutrons, neutron reaction cross-section, neutron sources, theory of activation analysis, activation equations, principle of standardization and geology of bauxite.

Chapter three discussed the materials and methodology under the following; sample collection, sample preparation, experimental set-up and experimental procedures.

Chapter four discussed the various results of chapter three.

Chapter five discussed the summary of the work, conclusion and recommendation.

5.2 CONCLUSION.

The energy calibration of the NaI (Tl)-detector used was done prior to all measurements. Absolute efficiency of the detector using gamma-energy standard point sources was found to be in the range 0 – 30%. Also the efficiency calibration of bulk sample was done for the NaI (Tl)-detector and was found to be in the range 0 – 28%.

The average Aluminiun concentration via ko-NAA using 5Ci Am – Be neutron source are 11.13±1.15%, 8.09±75% and 0.02±0.007% for the raw samples I, II and III respectively. These results compare well with the results of Reactor Nuclear Activation Analysis (RNAA) for raw samples I and

II. For raw sample III, the ko-NAA result shows a very low concentration while the RNAA result indicates that the Aluminium concentration is below the detection limit of the measuring facility. This also shows a good agreement.

The Aluminium – Silicon concentration ratios of this work (0.72±0.05, 0.98±0.14, 0.97±0.12, 0.70±0.11, 0.98±0.14, 0.59±0.03, 0.67±0.08, 0.57±0.08, 0.67±0.07, 0.84±0.05, 0.38±0.07, 0.41±0.01, 0.81±0.05, 1.30±0.25, 0.55±0.27) compare well with the Aluminium – Silicon weight ratios of Jonah, et al, 2004 for other samples.

Since there is good agreement in Aluminium concentration via ko-NAA using 5Ci Am – Be neutron source and that obtained from RNAA and also there is good agreement in Alumino-Silicate concentration ratios via ko-NAA and Alumino-Silicate weight ratios using the same 5Ci Am–Be neutron source, we therefore conclude that the ko-NAA determination of Alumino–Silicate ratio in bauxites or any other Alumino-Silicate ores is possible using 5Ci Am–Be neutron source.

5.3 LIMITATION AND RECOMMENDATION.

The Ko-NAA is suitable only for (n, γ) nuclear reactions. Determination of silicon concentration directly is a major limitation in Ko-NAA as there is no Ko- value for $^{28}Si(n,p)^{28}Al$ reaction. Also the RNAA can not give silicon concentration in any silicate ore. I therefore recommend that more research work should be done with 14MeV neutron generator on these samples to ascertain the silicon concentration contained in them and to establish further the Alumino- Silicate ratio obtained.

References

Acharya R.N., A.G.C., Reddy A.V.R., and Manohar S.B., (2002).validation of a Neutron Activation Analysis method using k_0-standardization, J. Appl. Rad and Isotop. Vol. 57 pp 391-398.

Ahmad K., Osae E.K., Amuh G., (1991) use of Am-Be Neutron source in Gold prospecting, IAEA-sm-308.

Aksoy, A., Al-Haddah, M.N., Naqvi, A.A and Al-Nahdi, K. (1994). ^{241}Am-Be Source Based Thermal Neutron Activation Analysis Facility at KFUPM. Journal of Radioanalytical and Nuclear Chemistry, Vol. 181, No.1, p131-140.

Alamin M.B. and Spyrou N.M., (1996) Semi-empirical Determination of Detector Absolute Efficiency in NAA of Voluminous Samples. Journal of Radioanalytical and nuclear Chemistry. Vol.184, No.1, p201-210.

BARC (1995). Reactor Neutron Activation Analysis by Single Comparator Method: K_0-Measurements, Bhabba Atomic Center Bombay, India. BARC/1195/E/007.

Batra R.J., Garg A.N., (1989) "Thermal neutron Activation Analysis of Cu in Its ores by using ^{241}Am-Be Neutron Source; Journal of Radioanalytical and Nuclear Chemistry; Vol: 129. No.2 pp 335-342.

Batra R.J., Lanjewa R.B., Garg A.N., (1986). NAA Determination of Iron and Silicon in USGS Standards and Bauxites Using Fast Neutrons from ^{241}Am-Be Source. Journal of Radioanalytical and Nuclear Chemistry. Vol.125, No.1 pp235-239

Breit G., Wigner E.P.(1936), Physical Review, J.Appl. Rad. And Isotop.Vol.49,pp 519.

De Corte F and Andras S (2003). Recommended Nuclear Data for use in the k_0-Standardization

of Neutron Activation Analysis. www.elsevier.com/locate/adt.P.47-67

De Corte, F. (1987) The k_0-Standardization method, A Move to the Optimization of Neutron Activation Analysis. Habiltation thesis, Gent Belgium.

Doulers, Y (1970). Thermal Neutrons. IAEA Technical Reports on Neutron Fluence Measurements. Series No. 107. P 45-47.

Evans R. D., (1982). The Atomic Nucleus. Krieger Press, New York.

GSN, (1974), Geological Map of Nigeria 1:2,000,000.

Gurna S.S. and Bhalla N.S., (IAEA, 1977). Neutron Activation Analysis of Tantalum in Ores and Concentrates Using Low level Isotopic Neutron Source. Prod. Of the Int. Symp. On Nuclear Techniques in Exploration, Extraction, and processing of Mineral Resources. Vienna, 7-10 March, 1977. P. 343-351.

Hoste J., (1988). Isotopic Neutron Source for Neutron Activation Analysis. IAEA-TEC DOC-465.

IAEA (1970). Neutron Fluence Measurements. Technical Report Series. No. 107. P 14.

Idris, Y.U (1998). Application of Nuclear Analytical Technique in Bauxite Ore Evaluation. Unpublished Ph.D Thesis, Ahmadu Bello University, Zaria, Nigeria.

Ila P., Marcfarlene A.M. (1994). Qualitative Determination of In and Sn in Cassiterites by Instrumental Neutron Activation Analysis. Journal of Radio Analytical and Nuclear Chemistry, Vol. 482. No. 2, P 427-435.

Isa, N. F. (2002). Analysis of Energy Minerals Using Thermalized Neutrons, Unpublished Ph.D

Dissertation, Physics Department, Ahmadu Bello University, Zaria. Nigeria.

Jonah, S.A., Oladipo, M. O.A., Umar, I.M., Rabiu, N., Idris, Y.U. and Zakari, I.Y. (2004). A Quick Method for the Determination of Al/Si Weight Ratio in Alumino-Silicates using an Am-Be Neutron Source. Journal of Radioanalytical and Nuclear Chemistry, Vol. 262, No. 2, p 501-504

Knoll, F. G., (1979). Radiation Detection and Measurement. Cambridge University Press, New York.

Mossop G.M. (1968). Advanced Level Atomic Physics. University of London Press Ltd. PP97.

Nell. N.G, Gian P.L (1993) Ore Deposit Models v.ii. Geoscience Canada Reprint series 6.

Onoja, A (1995) Application of Nuclear Analytical Techniques in Manganese Ore Evaluation, Unpublished Ph. D. thesis. Ahmadu Bello University Zaria, Nigeria.

Rabiu, N (2005) k_o-NAA Standardization of 5Ci Am-Be neutron source, Unpublished Ph.D. thesis Ahmadu Bello University, Zaria. Nigeria.

Ramos – lerate I., Barrera M., Ligero R.A., Casas-ruiz M., (1998). A new method for Gamma Efficiency Calibration of Voluminal Samples in Cylindrical Geometry. Journal of Environmental Radioactivity, Vol: 38 Nol, pp 47-57

Rieppo R., (1984) The Absolute Intensities of Am-Be Neutrons as a function of Neutron Energy Int. J. Appl. Radiation isotopes, Vol, 35, p41

Rieppo, R. (1983). The thermalization of Am-Be Neutrons in Paraffin.Int. J. Appl. Radiation isotopes. Vol. 34, p21.

Table4.14: The counts per second, the saturation, delay, counting factors and the specific activities (Asp) of the raw samples and the gold foil

Sam	W_{sam} (g)	Irrad site	$((cps)_{sam}$	S_{sam}	D_{sam}	C_{sam}	Asp(cps/g) Sam	W_{foil} (g)	$(cps)_{foil}$	S_{foil}	D_{foil}	C_{foil}	$(Asp)_{foil}$ (cps/g)
Ia	4.0	3	23.40±1.41	1	0.734	0.13	25.71±1.55	0.0789	17.35±0.98	0.011	1.0	1.0	19992.58±1129.23
Ib	»	4	22.76±1.42	»	»	»	25.01±1.56	0.0786	15.75±1.13	0.011	1.0	1.0	18221.72±1307.34
Ic	»	5	23.56±1.41	»	»	»	28.89±1.55	0.0790	17.75±1.35	0.011	1.0	1.0	20430.27±1553.85
Id	»	6	24.71±1.75	»	»	»	27.15±1.92	0.0787	19.46±1.53	0.011	1.0	1.0	22481.66±1767.57
IIa	»	1	17.68±1.10	»	»	»	19.32±1.20	0.0789	19.70±1.02	0.011	1.0	1.0	22699.53±1144.24
IIb	»	5	16.75±0.90	»	»	»	18.49±0.99	0.0791	16.61±1.48	0.011	1.0	1.0	19085.62±1700.59
IIc	»	2	17.33±1.18	»	»	»	19.04±1.30	0.0786	18.65±1.60	0.011	1.0	1.0	21570.58±1850.56
IId	»	3	16.97±0.61	»	»	»	18.65±0.69	0.0792	17.27±1.27	0.011	1.0	1.0	19818.78±1457.43
IIIa	»	4	0.046±0.008	»	»	»	0.05±0.009	0.0788	18.62±1.28	0.011	1.0	1.0	21476.11±1525.50
IIIb	»	3	0.055±0.010	»	»	»	0.06±0.01	0.0788	16.61±1.67	0.011	1.0	1.0	19167.12±1927.10
IIIc	»	6	0.036±0.012	»	»	»	0.04±0.013	0.0789	19.40±1.34	0.011	1.0	1.0	20051.91±1385.03
IIId	»	5	0.055±0.008	»	»	»	0.06±0.009	0.0788	16.47±1.02	0.011	1.0	1.0	18997.43±1176.53

Table 4.15: Nuclear data used in the calculation (De-Corte, 1987)

Nuclear reaction	Half life	$E\gamma$(KeV)	Qo	Isot. abund (%)	K_o-value	Ë(eV)
$^{197}Au(n,\gamma)^{198}Au$	2.7days	411.8	15.69	95.53	1.00	5.65
$^{27}Al(n,\gamma)^{28}Al$	2.24mins	1778.9	0.74	100	0.0179	11800

Table 4.16: Values of α and the flux ratios,f used in the calculation (Rabiu, 2005)

Irrad site	1	2	3	4	5	6
α	-0.32653	-0.43572	-0.41736	-0.41885	-0.44270	-0.32759
F	146.09	258.59	202.22	203.93	242.81	147.21

Table4.17: Aluminum concentration in part per million (ppm) of the raw samples via Ko-NAA Technique

Sample no	Sample Type	Irrad site	Asp,a (cps/g)	Asp,m (cps/g)	F	Qo,a (α)	Qo,m (α)	Ko,m	Ep,a (%)	Ep,m (%)	Al-conc (ppm)
Ia	Al-ore	3	25.71±1.55	19992.55±1129.23	202.22	17.59	33.50	0.0179	11.35	16.50	12000±13046
Ib	Al-ore	4	25.01±1.56	18221.72±1307.34	203.94	17.84	33.58	0.0179	11.35	16.50	114231± 15277
Ic	Al-ore	5	25.89±1.55	20430.27±1553.85	242.81	22. 61	35.72	0.0179	11.35	16.50	107998±14693
Id	Al-ore	6	27.15±1.92	22481.66±1787.57	147.21	7. 73	27.93	0.0179	11.35	16.50	110866±16588
IIa	Al-ore	1	19.32±1.20	22699.53±1144.24	146.09	7. 66	27.88	0.0179	11.35	16.50	78214±8791
IIb	Al-ore	5	18.49±0.99	19085.62 ±1700.59	242.81	22.61	35.72	0.0179	11.35	16.50	82573±11816
IIc	Al-ore	2	19.04±1.30	21570.58±1850.56	258.59	21.06	35.02	0.0179	11.35	16.50	80752±12419
IId	Al-ore	3	18.65±0.67	19818.78±1457.43	202.22	17.59	35.50	0.0179	11.35	16.50	81957±8977
IIIa	Al-ore	4	0.05±0.009	21476.11±1525.50	203.93	17.84	33.58	0.0179	11.35	16.50	203±50
IIIb	Al-ore	3	0.06±0.01	19167.12±1927.10	202.22	17.59	33.50	0.0179	11.35	16.50	273±73
IIIc	Al-ore	6	0.04±0.013	20051.91±1385.03	147.21	7. 73	27.93	0.0179	11.35	16.50	183±72
IIId	Al-ore	5	0.06±0.009	18997.43±1176.53	242.81	22.61	35.72	0.0179	11.35	16.50	269±57

Table4.18: The counts per second (cps),the saturation, decay, counting factor and the specific activities (Asp) of other samples and the foils attached when irradiated bared .

Sample	W(g) Sam	Irrad Site	CPS sam	S sam	D sam	C sam	Asp sample	W(g) foil	CPS foil	S foil	D foil	C foil	Asp foil
Bau 1	3.001	4	0.064±0.013	1	0.734	0.31	0.281±0.057	0.0786	19.23±1.15	0.011	1.0	1.0	22236.00±1330
Bau 2	3.000	3	0.078±0.012	»	»	»	0.342±0.053	0.0789	19.02±1.18	»	»	»	21911.12±1359
Bau 3	3.004	1	0.086±0.013	»	»	»	0.379±0.062	0.0787	18.63±1.35	»	»	»	21521.72±1560
Bau 4	3.002	2	0.070±0.012	»	»	»	0.306±0.052	0.0790	18.84±1.37	»	»	»	21677.80±1576
Bau 5	3.001	5	0.097±0.013	»	»	»	0.426±0.057	0.0788	18.69±1.18	»	»	»	21560.11±1361
Ben 1	3.001	6	0.115±0.012	»	»	»	0.506±0.053	0.0789	18.32±1.45	»	»	»	21110.67±1670
Ben 2	3.000	3	0.104±0.012	»	»	»	0.456±0.053	0.0788	19.11±1.33	»	»	»	22051.30±1535
Ben 3	3.003	4	0.111±0.015	»	»	»	0.499±0.067	0.0791	19.30±1.01	»	»	»	22180.71±1160
Ben 4	3.003	2	0.14±0.010	»	»	»	0.620±0.044	0.0789	19.07±1.22	»	»	»	21968.31±1405
Clay b	3.000	1	0.164±0.013	»	»	»	0.719±0.057	0.0788	18.80±1.13	»	»	»	21691.40±1303
Felds p	3.001	5	0.134±0.012	»	»	»	0.587±0.053	0.0786	18.92±1.33	»	»	»	21881.20±1538
Kaolin	3.001	6	0.047±0.012	»	»	»	0.208±0.053	0.0787	19.12±1.18	»	»	»	22090.31±1363
S_1	3.002	3	0.138±0.013	»	»	»	0.607±0.057	0.0789	19.22±1.12	»	»	»	22150.63±1291
S_2	3.001	4	0.100±0.013	»	»	»	0.440±0.057	0.0788	19.03±1.15	»	»	»	21958.12±1327
S_3	3.002	2	0.058± 0.013	»	»	»	0.253±0.057	0.0790	18.80±1.03	»	»	»	21630.50±1185

S_1 =60%Al_2O_3 + 40% SiO_2

S_2 =40%Al_2O_3 + 60% SiO_2

S_3 =BCS-CRM 348.

Table4.19: Aluminum concentration via Ko-NAA Technique of other sample

Sample	Irrad site	Asp a Ep,a (%)	Asp,m Ep,m (%)	F	Qo,a (α)	Qo,m (α)	Ko,m Al-conc (ppm
Bau 1	4	0.281±0.057	22236.00±1330	203.93	17.84	33.58	0.0179
	11.35	16.50	1098.49±288				
Bau 2	3	0.342±0.053	21911.12±1359	202.22	17.59	33.50	»
Bau 3	1	0.379±0.062	21521.72±1560	146.09	7. 66	27.88	»
Bau 4	2	0.306±0.052	21677.80±1576	258.59	21.06	35.02	»
Bau 5	5	0.426±0.057	21560.11±1361	242.81	22.61	35.72	»
Ben 1	6	0.506 ±0.053	21110.67±1670	147.21	7. 73	27.93	»
Ben 2	3	0.456±0.053	22051.30±1535	202.22	17.59	33.50	»
Ben 3	4	0.499±0.067	22180.71±1160	203.93	17.84	33.58	»
Ben 4	2	0.620±0.044	21968.31±1405	258.59	21.06	35.02	»
Clayball	1	0.719±0.057	21691.40±1303	146.09	7. 66	27.88	»
Fedspar	5	0.587±0.053	21881.20±1538	242.81	22.61	35.72	»
Kaolin	6	0.208±0.053	22090.31±1363	147.21	7. 73	27.93	»
S_1	3	0.607±0.057	22150.63±1291	202.22	17.59	33.50	»
S_2	4	0.440±0.057	21958.12±1327	203.93	17.84	33.58	»
S_3	2	0.253±0.057	21630.50±1185	258.59	21.06	35.02	»

Table4.20: Peak counts (Bare and cd-cover) of 40% Al_2O_3+ 60% SiO_2 and 60% Al_2O_3+ 40% SiO_2 in each irradiation site.

	Irradiation site	1	2	3	4	5	6
Peak counts (60%Al_2O_3 +40%SiO_2)	Bare	1161±128	1155±130	1149±136	1151±812	1157±129	1140±130
	cd-cover	640±120	639±122	645±126	630±129	625±130	629±128
Peak counts	Bare	1170±131	1163±130	115±125	1161±128	1160±118	1145±125

(40%Al_2O_3 +60%SiO_2)	cd-cover	477±122	470±122	477±120	471±132	400±130	465±127
...							

Table4.21: Neutron flux distribution of the six irradiation sites of the Am-Be neutron source used in this work (Rabiu, 2005)

Irradiation site	1	2	3	4	5	6
Fast Neutron flux	$5.54x10^4$	$4.64x10^4$	$5.58x10^4$	$4.76x10^4$	$4.00x10^4$	$4.57x10^4$
Thermal neutron flux	$1.39x10^4$	$1.36x10^4$	$1.25x10^4$	$1.20x10^4$	$1.36x10^4$	$1.16x10^4$

Table4.22: Values of K for the six irradiation sites. Where K* and K** are the values of K determined using the peak counts

(bare and Cd-corer) of 40% Al_2O_3 + 60% SiO_2 and 60% Al_2O_3 + 40% SiO_2 respectively.

Irrad site	K^x	K^{xx}
1	0.23	0.29
2	0.27	0.34
3	0.22	0.27
4	0.25	0.31
5	0.30	0.30
6	0.24	0.29

Table4.23: Results of silicon concentration using the valves of k (k_{Call} and $k_{exp\,t}$) and the concentration obtained via Ko-NAA of the raw samples.

Sample	Irrad	$(Np)_{Al}$	$(Np)_{Si}$	$Ø_{fast}$	$Ø_{thermal}$	Al-conc	$(Si\text{-}conc)_{cal}$	$(Si\text{-}conc)_{exp}$	Al-conc	Al-conc

Site							
					$\times 10^4$	$\times 10^4$	(ppm)	(ppm)
Ia	3	23.40±1.41	5.60±0.94	5.58	1.25	112000±13046	25018±8647
21444±9687		4.48±0.46	5.22±0.57				
Ib	4	22.76±1.42	5.29±0.97	4.76	1.28	114231±15277	29748±7473
25498±9867		3.38±0.38	4.48±0.52				
Ic	5	23.56±1.41	5.47±0.99	4.00	1.36	107998±14693	35522±8290
30447±10110		3.04±0.37	3.55±0.47				
Id	6	24.71±1.75	5.49±0.88	4.57	1.16	110866±16588	26051±8791
22330±9210		4.26±0.49	4.96±0.56				
IIa	1	17.68±1.10	3.61±0.8	5.54	1.39	78214±8791	16696±6611
14311±4300		4.68±0.51	5.47±0.41				
IIb	5	16.75±0.90	4.64±0.6	4.00	1.36	82573±11816	32405±9231
27776±9921		2.55±0.43	2.97±0.50				
IIc	2	17.33±1.18	3.79±0.98	4.64	1.35	80752±12419	21568±7101
18487±4210		3.74±0.48	4.37±0.38				
IId	3	16.97±0.61	5.00±0.35	5.58	1.25	81957±8977	22539±7566
19319±4561		3.64±0.46	4.24±0.35				
IIIa	4	0.046±0.008	5.77±0.42	4.76	1.28	203±50	28530±10059
24455±6107		0.007±0.001	0.008±0.0005				
IIIb	3	0.055±0.010	5.84±0.4	5.58	1.25	273±73	27057±9230
23192±5921		0.010±0.003	0.011±0.003				
IIIc	6	0.036±0.012	5.56±0.38	4.57	1.16	183±72	29892±10050
25622±6510		0.006±0.0014	0.007±0.0008				
IIId	5	0.055±0.008	6.01±0.37	4.00	1.36	269±57	41642±12800
35693±7980		0.006±0.0018	0.007±0.0004				

(ppm)	$(Si\text{-}conc)_{cal}$	$(Siconc)_{exp}$

Table4.24: Results of silicon concentrations using the two valves of K (K_{call}=0.24 and K_{exp} = 0.28 ± 0.3)
and Al – to - Si ratios of other samples.

Sample Site	Irrad	$(Np)_{Al}$ $\times 10^4$	$(Np)_{Si}$ $\times 10^4$	Øfast (ppm)	Øthermal (ppm)	Al-conc (ppm)	(Si-conc)cal	(Si-conc)exp	Al-conc (ppm)	Al-conc (Si-conc)cal	(Si-conc)exp

Bau 1	4	38±8	55±15	4.76	1.28	1098.49±288	1781.42±326
	1526.93±312		0.62±0.05	0.72±0.05			
Bau 2	3	47±7	60±15	5.58	1.25	1357.79±295	1617.90±301
	1386.77±298		0.84±0.02	0.98±0.14			
Bau 3	1	52±8	60±16	5.54	1.39	1620.40±382	1954.62±350
	1675.39±341		0.83±0.05	0.97±0.12			
Bau 4	2	42±7	57±13	4.64	1.36	1202.80±291	1993.56±401
	1708.76±376		0.60±0.03	0.70±0.11			
Bau 5	5	58±8	49±15	4.00	1.36	1683.35±331	2014.70±506
	1726.88±438		0.84 ±0.22	0.98±0.19			
Bent1	6	69±7	128±13	4.57	1.16	2198.78±404	4313.93±892
	3697.66±733		0.51±0.05	0.59±0.03			
Bent2	3	62±7	116±16	5.58	1.25	1801.27±335	3145.64±800
	2696.27±635		0.57±0.04	0.67±0.08			
Bent3	4	67±9	128±17	4.76	1.28	1957.30±365	4026.05±760
	3450.90±581		0.49±0.05	0.57±0.08			
Bent4	2	85±6	122±12	4.64	1.36	2404.64±324	4215.03±791
	3612.88±602		0.57±0.08	0.67±0.07			
Claybal	1	98±8	130±18	5.54	1.39	3044.20±424	4221.67±821
	3618.57±623		0.72±0.04	0.84±0.05			
Fedspa	5	80±7	176±16	4.00	1.36	2287.16±367	7128.32±901
	6109.98±750		0.32± 0.09	0.38±0.07			
Kaolin	6	28±7	76±12	4.57	1.16	866.04±274	2486.13±358
	2130.97±342		0.35±0.02	0.41±0.01			
S_1	3	83±8	57±16	5.58	1.25	2386.40±363	1529.69±279
	1835.63±290		1.56±0.02	1.30±0.25			
S_2	4	60±9	77±15	4.76	1.28	1744.76±331	2508.81±682
	2150.40±530		0.70±0.09	0.81±0.05			
S_3	2	35±8	61±17	4.64	1.36	998.90±279	2126.15±341
	1822.41±480		0.47±0.29	0.55±0.27			